

A WIRELESS SENSORIZED INSOLE FOR GAIT QUANTIFICATION

A Dissertation for fulfillment of the requirements for the Degree

of

MASTER OF ENGINEERING

in

Electronic Instrumentation & Control Engineering

submitted by

Abhinandan Aggarwal

Reg. No. 801651001

under the Guidance of

Dr. Ravinder Agarwal

Professor, EIED

Thapar Institute of Engineering & Technology

Patiala



Electrical and Instrumentation Engineering Department

Thapar Institute of Engineering & Technology, Patiala

(Declared as Deemed-to-be-University u/s 3 of the UGC Act., 1956)

Post Bag No. 32, Patiala – 147004

June, 2018

DECLARATION

I hereby certify that the work which is presented in this dissertation entitled, “**A Wireless Sensorized Insole for Gait Quantification**”, in complete fulfilment of the requirements for the award of the degree of Master of Engineering in Electronic Instrumentation and Control Engineering, submitted to Electrical & Instrumentation Engineering Department of TIET, Patiala is as authentic record of my own work carried under the supervision of Dr. Ravinder Agarwal. It refers others researcher’s work which is duly listed in the reference section. The matter contained in this dissertation has not been submitted, neither in part nor in full to any other degree to any other university or institute except as reported in the text and references.

Place: Patiala
Date: June 29, 2018

Abhinandan
(Abhinandan Aggarwal)
Roll No.: 801651001

It is certified that the above statement made by the student is correct to the best of my knowledge and belief.

Date: June 29, 2018

Agarwal
(Dr. Ravinder Agarwal)
Professor
Electrical & Instrumentation Engineering Department
Thapar Institute of Engineering & Technology, Patiala

ACKNOWLEDGEMENT

I am grateful to my M.E. dissertation supervisor **Dr. Ravinder Agarwal, Professor**, Department of Electrical and Instrumentation Engineering, TIET, Patiala, whose help, stimulating suggestions and encouragement helped me in all the time of research for and writing of this dissertation. I am deeply indebted to him for his dynamic support, keen interest and special attention during the entire stretch of research pursuit. I could not have imagined having a better advisor and mentor for my M.E. dissertation.

I am also highly thankful to **Dr. R. S. Kaler**, Head, **Dr. Nirbhowjap Singh**, P.G.Coordinator of M.E. (EIC), and my venerable teachers, Department of Electrical and Instrumentation Engineering, TIET, Patiala for their invaluable suggestions and caring concern at every stage during the entire studies.

My heartiest thanks are due to all lab members of Biomedical Research Lab for all help rendered to me besides taking personal pains to see the completion of my research. I am immensely thankful to them for reviewing and assessing the progress of my research work and also for their valuable suggestions to augment the quality of my work. I am also highly thankful technical staff Thapar Institute for their personal support and constant encouragement.

Finally, I express my deepest feeling of gratitude and I pay my best regards to my parents who provided the best for me in my life. Also, I express my sincere gratitude to my friends Ravi, Kamlesh and Nishant for their generous help and continuous support.

Thank you all for your insights, guidance and support.

Abhinandan

(Abhinandan Aggarwal)

CONTENTS

DECLARATION	i
ACKNOWLEDGEMENT	ii
LIST OF FIGURES.....	v
LIST OF TABLES.....	vi
ABSTRACT	vii
Chapter 1 : INTRODUCTION	1
1.1 Gait Introduction.....	1
1.2 Gait Analysis Methods	3
1.2.1 Observation based.....	3
1.2.2 Camera based.....	4
1.2.3 Electromyography.....	5
1.2.4 Force plates.....	5
1.2.5 Systems using inertia.....	5
1.2.6 Plantar pressure insoles.....	6
1.3 Need of Insoles	7
Chapter 2 : LITERATURE SURVEY	9
Chapter 3 : MATERIALS AND METHODS.....	13
3.1 Premise	13
3.2 Experimental Protocol	14
3.3 Precautions.....	14
3.4 Communication Protocol Trials.....	15
3.4.1 Communication using WiFi module.....	15
3.4.2 Communication using Bluetooth module	16
3.4.3 Communication using RF module	16
3.5 Data Communication Module Construction.....	18
3.5.1 CD74HC4067	18
3.5.2 Arduino Nano	19
3.5.3 Interlink force sensitive resistor.....	20
3.5.4 Nordic nRF24I01+	21
3.6 Parameters Calculated	22
3.7 Sensors Localization.....	24
3.8 Complete Hardware Device.....	24
Chapter 4 : RESULTS AND DISCUSSIONS.....	26
4.1 Outcomes	26
Chapter 5 : CONCLUSION AND FUTURE SCOPE.....	33

5.1 Conclusion	33
5.2 Future Scope	33
LIST OF PUBLICATIONS	35
REFERENCES	36
ANNEXURE	39

LIST OF FIGURES

Figure 1.1: Gait Cycle/Stride	1
Figure 1.2: Gait Cycle Division	1
Figure 1.3: Normal Gait Cycle.....	2
Figure 1.4: Spatial Parameters	3
Figure 1.5: Optical Motion Tracking System	4
Figure 1.6: EMG Signal Corresponding to Gait	5
Figure 1.7: Inertial Measurement Unit.....	6
Figure 1.8: Insole Planter Pressure Measuring System.....	6
Figure 1.9: Insole with Multiple Sensors	7
Figure 3.1: Distance/Path Measurement and Marker Placement:	13
Figure 3.2: Communication using WiFi Module	15
Figure 3.3: Communication using Bluetooth Module.....	16
Figure 3.4: Basic Block Diagram.....	17
Figure 3.5: Communication using RF Module	17
Figure 3.6: Analog Multiplexer	19
Figure 3.7: Arduino Nano	19
Figure 3.8: FSR Response Curves	20
Figure 3.9: FSR Sensor	21
Figure 3.10: NRF24L01 RF Module.....	22
Figure 3.11: Sensor Locations	24
Figure 3.12: Complete Device with Insoles.....	24
Figure 3.13: Subject Wearing the Insoles in Left (Red LED) and Right (Green LED) foot	25
Figure 3.14: Generic Sensor Placement on the Left Insole.....	25
Figure 4.1: Trial Data for Left Foot	27
Figure 4.2: Trial Data for Right Foot.....	28
Figure 4.3: Centre of Pressure Plots for Left Foot for Subject 2	29
Figure 4.4: Centre of Pressure Plots for Right Foot for Subject 2	29
Figure 4.5: Centre of Pressure Plots for Both Feet for Subject 2.....	30
Figure 4.6: Centre of Pressure Plots for Both Feet for Subject 1.....	30
Figure 4.7: Centre of Pressure Plots for Both Feet for Subject 3.....	31
Figure 4.8: Centre of Pressure Plots for Both Feet for Subject 5.....	31
Figure 4.9: Centre of Pressure Plots for Both Feet for Subject 4.....	32

LIST OF TABLES

Table 3.1: Parameter used.....	23
Table 4.1: Parameter Table for 12 Meter Path Trials.....	26
Table 4.2: Parameter Table for 16 Meter Path Trials.....	26
Table 4.3: Parameter Table for 20 Meter Path Trials.....	26

ABSTRACT

A wireless footwear insole is developed, which is useful in data acquisition and analysis of gait parameters. Regular assessing is essential to examine the quality of gait before, after and during rehabilitation. Footgear systems are quite a common choice for investigators as they are non-invasive with consumer friendly setup. The apparatus designed here, investigates gait patterns by using FSR type pressure sensing elements, integrated within the shoe insole. The positioning of the sensors were marked by capturing the footprint of the subject in a sandbox and then indicating the depressions. The sensors logged the data during each step and parameters were obtained from the data by performing post processing. Experiments were carried out, to validate the reliability of the obtained data by the developed insole system and the efficiency of the algorithm to calculate the parameters. A symmetry has been observed in the case of healthy subjects in terms of alike step lengths, stride lengths, velocities and centre of pressure trajectories. A wireless pressure-sensor-based insole system is developed to observe gait parameters and critical occurrences. The device is used to calculate various parameters for five subjects for different path lengths of 12 m, 16 m and 20 m.

Keywords: Footwear; Gait; Insoles; Force Sensitive Resistors; Wireless

Chapter 1 : INTRODUCTION

1.1 Gait Introduction

During the motion of body, leg (limb) acts similar to the body movement (forward), one limb serves as a motile source of backing/support while the other leg approaches to a new support site. Then the legs reverse their roles. During the redistribution of body weight both the feet are on ground. Repetition of these events is undertaken until the point of target is reached. An individual sequence of this activity is known as Gait Cycle [1] as shown in Figure 1.1.

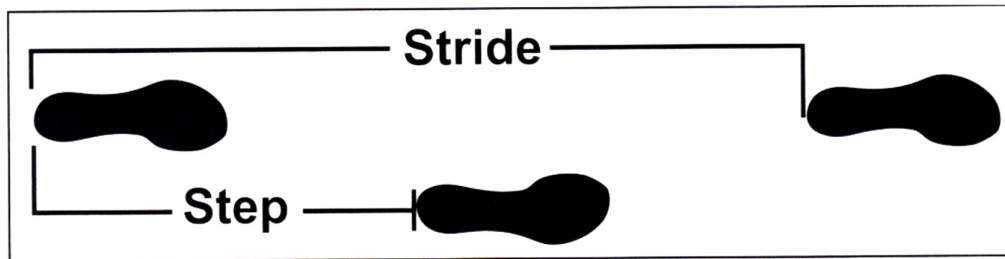


Figure 1.1: Gait Cycle/Stride

Normal people begin floor connection with a Heel Strike (HS). Many people might not have this capability therefore a general term initial contact is used to specify the onset of gait cycle. The result of gait cycle is the centre of gravity being progressed forward. Gait cycle is also known as **Stride** in some texts. Time period from one event of one foot to following occurrence of the same event with the same foot can be termed as gait cycle in general [2]. In general the gait cycle is divided into two main periods i.e. the stance period and the swing period as described in the Figure 1.2.

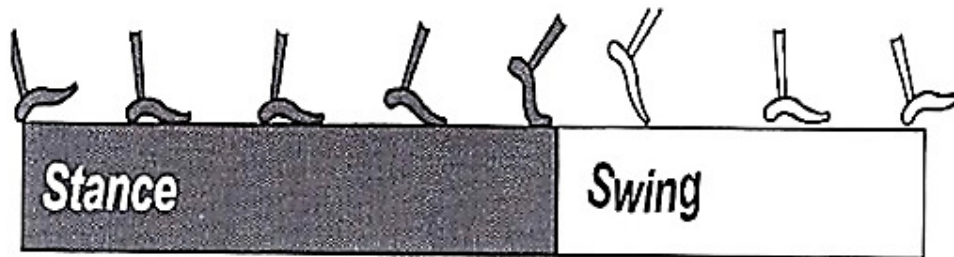


Figure 1.2: Gait Cycle Division

Stance period is the entire time when the foot is on the ground and the swing period is the time when the same foot is in air to advance the limb. This period begins as soon as the foot is lifted off the floor. Stance is further divided into five phases and accordingly swing period can also be divided in to three phases. The complete gait cycle for a normal person/ boy is

shown in Figure 1.3 with all the different phases in both stance and swing time period (included).

First double support is in stance phase is when both the feet are on ground contact. In single limb stance, right foot is in ground contact and the left foot is swinging. Second double support time is when both the feet are on ground again. Generally, there is a degree of symmetry in gait pattern between right and left side but, pathological imbalances might lead to variation in gait pattern particularly in swing phase and stance phase [3]. In a disability, the patient is prone to increase the stance time on the sound leg and its swing time will decrease. Similarly, the swing time on the painful leg will increase and the stance time will decrease [4].

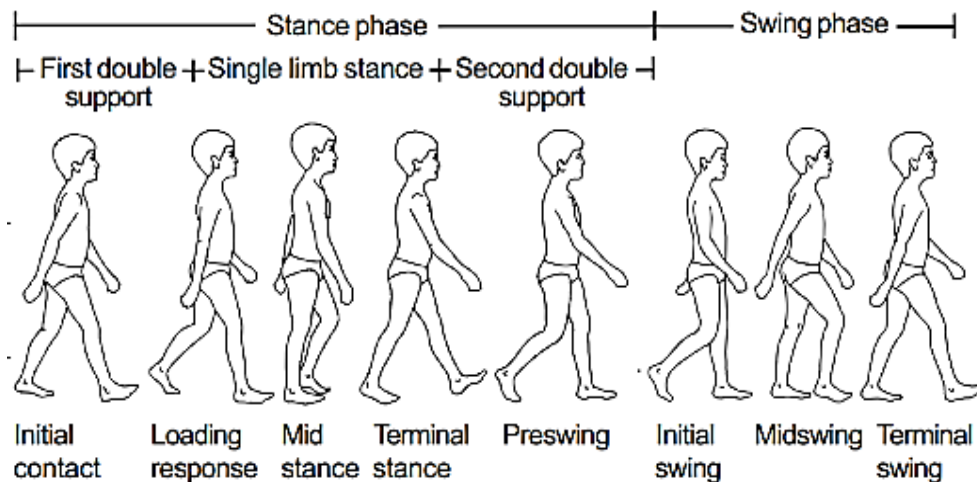


Figure 1.3: Normal Gait Cycle

Normal gait cycle has been divided into eight sub parts or sub-events starting form HS / initial contact which initialises the gait cycle. After HS the foot flat phase or loading response starts in which the plantar surface of the foot comes in contact with the ground. The next phase is mid-stance, in which the non-stationary foot crosses the stationary foot, leading to the next event of terminal stance or heel off. In this, the heel of the stationary foot loses contact with the ground a push-off is initiated. Heel off is followed by the starting of the pre-swing phase. In this, the toes of the contact foot leave the ground and the forward acceleration begins leading to the initial swing phase in which the next foot comes in contact with the ground. The next phase is mid swing phase. The foot passes directly beneath the body, coincidental with mid stance for the other foot. It is followed by the terminal swing in which the swing foot decelerates and the contact foot prepares for the next

step. Gait parameters can also be classified on the basis of temporal, spatial parameters which can be measured with different methods. The temporal parameters are related with time, for example, the percentage of time the different phases of the gait cover that lead to a full gait cycle and these timings vary comfortably in case of subjects with medical disability. The spatial parameters cover features like stride length, step length, step width *etc.* as can be seen in Figure 1.4.

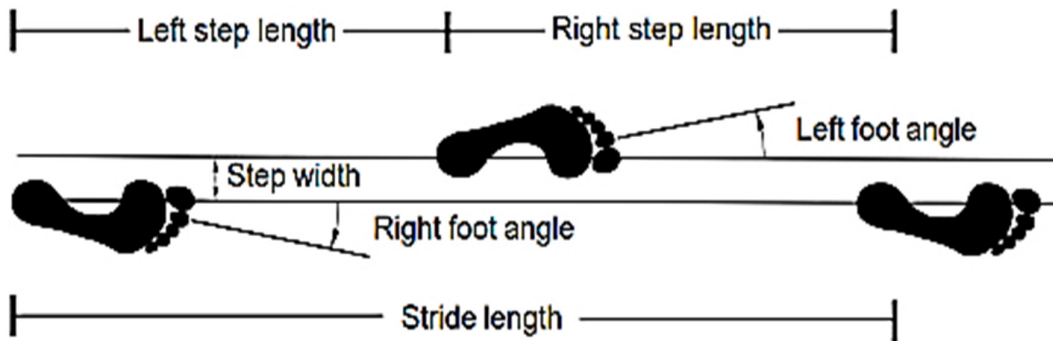


Figure 1.4: Spatial Parameters

The distance travelled by a subject in one gait cycle is known as stride length and is generally measured from HS of one foot to the next HS of the same foot. It can also be visualised as the sum of two step lengths. These parameters are similar in for a normal person's gait whereas a certain amount of deviation can be seen in a subject with any abnormality as described in the case of degenerative arthritis [5]. Step Width is another parameter which is one deciding factor during gait variability studies. Certain cases with cerebral palsy have been noticed with step width variability [3].

1.2 Gait Analysis Methods

1.2.1 Observation based

The concept of gait analysis has been prevalent since long time [6]. But due to the advent of modern computers the computational analysis and the diagnosis of gait related studies have grown by leaps and bounds. A qualitative way to analyse gait clinically is through observation of the specific body sections such as trunk, pelvis and other extremities during walking. Few advantages of using gait analysis via observation are simple, rapid and low cost as compared to other technical methods of analysis. Moreover, techniques such as slow motion replay freeze the frame aid in analysis than unaided observation through visualisation. This way of observation is highly subjective in nature thereby leading to poor

reliability, sensitivity, doubtful validity in comparison with gait analysis with instruments [7, 8]. Therefore, the clinicians are expected to be experts in their observational skills to correctly assess the gait data.

1.2.2 Camera based

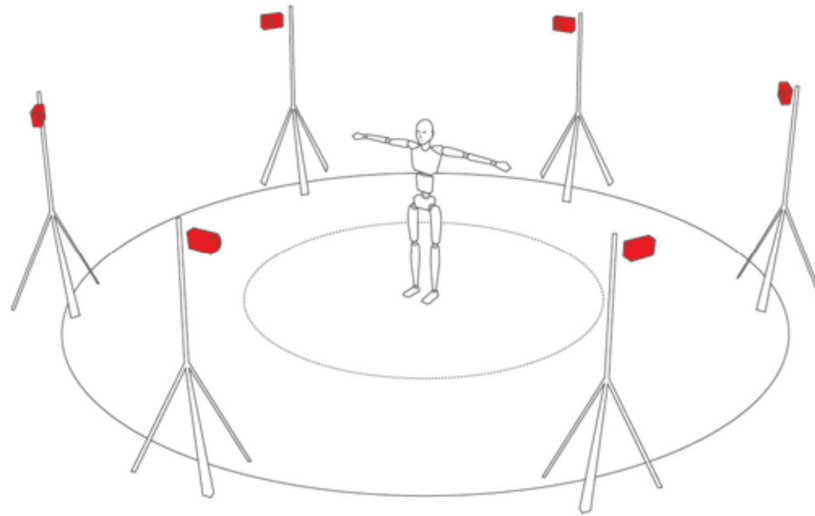


Figure 1.5: Optical Motion Tracking System

The techniques used to observe gait are categorised in two major segments of with markers and without markers. Motion capture is done using the cameras (Figure 1.5) for a subject to quantify the gait parameters. For the motion analysis, in two dimensions, one camera is required positioned perpendicular to the plane of motion and for the three dimension analysis two or more cameras are required to quantise the data in all planes of motion. In the optoelectronic systems [9, 10] the data sampling rate vary from 50-1000 Hz and a 60 Hz sampling rate is sufficient for the gait analysis of a subject. It is suggested in [11] that most of the body movements are well restricted to a frequency range of 15 Hz or below.

Tight costumes for marker placement and requirement of expensive equipment may pose difficulties during efficient recording and analysing the data during gait monitoring experiments. In case of motions involving movement of lower extremity produces appreciable results still it is not easily accessible and is restricted to lab environment.

1.2.3 Electromyography

Detection, measurement and recording of minute electric impulses produced inside a muscle during various types of activities is known as electromyography [12]. The electrodes can either be placed in the skin surface or placed inside the target muscle [13].

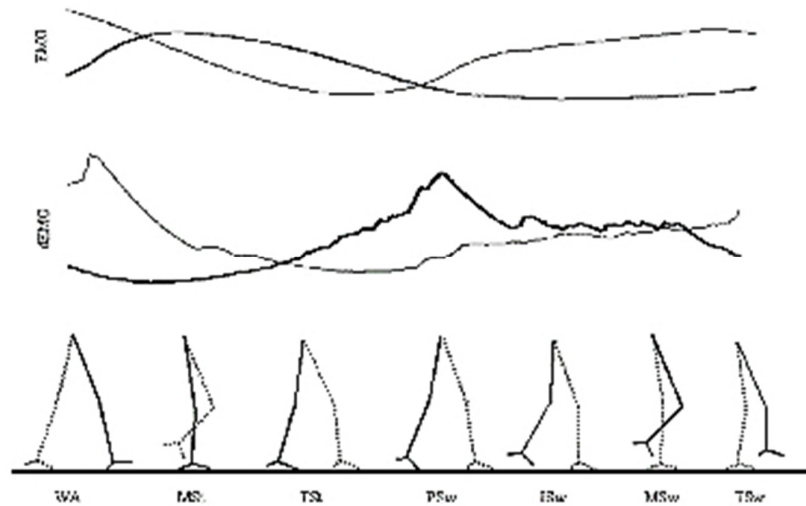


Figure 1.6: EMG Signal Corresponding to Gait

Figure 1.6 shows that the variation in EMG signal is quite prominent and data can be extracted. Although, the data quality is not appreciable as the sensors are not only detecting the motion signals but a lot of artefact/ noise which is present around the sensor. Here, due to considerably high sensitivity, crosstalk is inserted in the data from the muscles around the target muscle. Although by inserting the electrode inside the muscle there is improvement in the signal/data quality [14].

1.2.4 Force plates

Generally, force plates consist of two steel plates with transducers sandwiched between them and whenever any kind of force is applied the load is converted into an electrical signal. The force vector can be easily calculated instantaneously including the centre of pressure. The biomechanical measures for single foot strike can be calculated by the force plates [15]. This system is implemented in addition to the motion capture system.

1.2.5 Systems using inertia

The tendency of an object to resist the change in position is used in these systems. It is also known as moment of inertia. Contemporary technologies use accelerometer, magnetometer

and gyroscope in a single product to measure the differential parameters as shown in Figure 1.7. Now-a-days the combination of these three sensors is called IMU. Although, these sensors are very noisy, they can record data for hours before draining out the battery due to low current consumption [16].

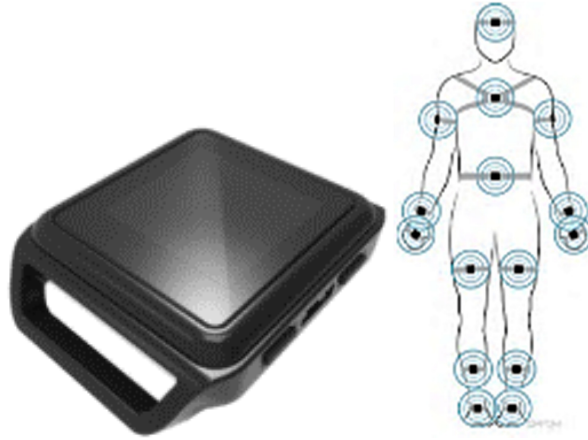


Figure 1.7: Inertial Measurement Unit

1.2.6 Plantar pressure insoles

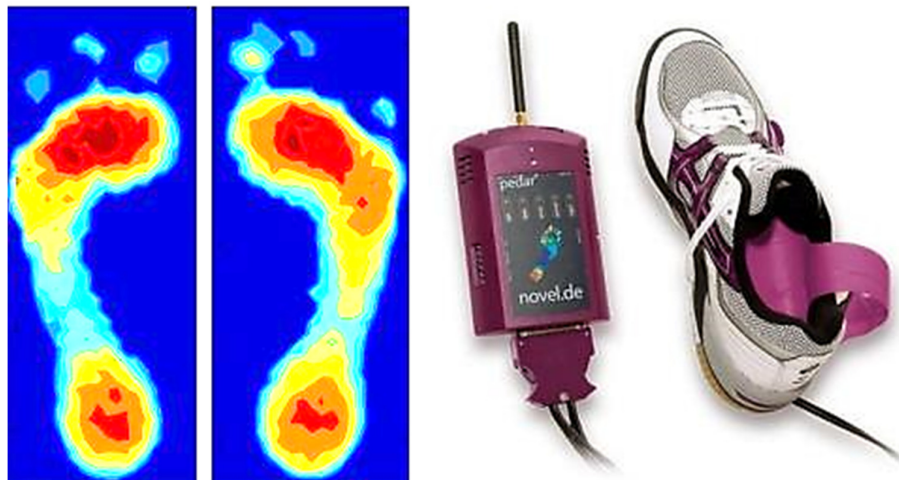


Figure 1.8: Insole Planter Pressure Measuring System

These types of insoles measure the amount of pressure being put on them. These insoles are embedded with numerous pressure sensors to track gait parameters effectively as shown in Figure 1.8. The parameters measured are both in space and in time i.e. Spatio-Temporal manner [17]. The gait parameters were monitored simultaneously and the data acquired was used for post processing.

1.3 Need of Insoles

The contemporary technologies require more resources such as equipment training, analyse data, time to collect, cost *etc.* and are not clinic friendly. However, a wireless insole system is advantageous as, it provides real time information in addition to minimal resources. It helps to analyse and monitor the gait abnormalities and strive towards a healthier gait and for rehabilitation in transtibial amputees.

Various types of insole systems are available in the market as well as in the laboratories which differ in design and instrumentation. The key parameters taken care of in any design were the size, weight, energy efficiency, sensitivity, cost, calibration, sampling frequency, *etc.* The sensor selection was also one key parameter which includes repeatability, durability, linearity, size, *etc.* Gait parameters were extracted reliably using pressure sensitive insoles where sensor placement plays a crucial role in data acquisition. The pressure bearing points on the foot need to be located, to get the maximum amount of data associated with gait. Few commercial footprint measuring products [18] like Shustrack System, Microcapsule Socks, Pressuresat Film were available easily to locate the sensor positions.

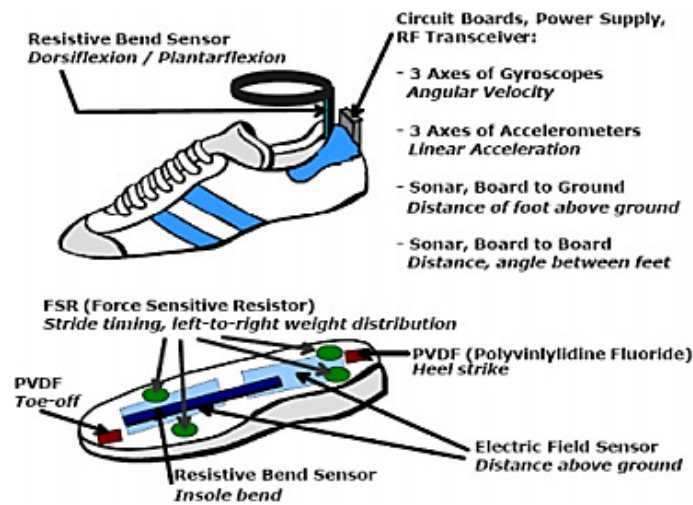


Figure 1.9: Insole with Multiple Sensors

Figure 1.9 shows a typical example of smart insole embedded with multiple sensors to record and extract multiple data parameters. An IMU which has an accelerometer, a gyroscope and a sonar module integrated in addition to FSR's PVDF strips, flex sensors and electric field height sensor [19]. It was later found that, too many sensors was an overkill for such application and were replaced with only two FSR sensors [20]. With this type of

system one cannot differentiate between pressure distribution between lateral and medial side foot. It makes difficult to determine amputee deviations like lateral and medial whip. The quality of data completely depends upon the location of pressure sensors. So, it should be distributed on the insole at the particular locations, where it can collect the maximum data and do not alter the gait of the person by causing discomfort during walking. Subjects with transtibial amputation stress the intact limb more, leading to secondary complications affecting the quality of life and mobility [5].

Chapter 2 : LITERATURE SURVEY

Bamberg *et al.* [19] described a wearable system to provide analysis of gait parameters using three accelerometers, three gyroscopes, two bend sensors, two pressure sensors, and height sensors using electric field. The sampling frequency on which the device acquired the data was 75 Hz. The data being acquired was transmitted to the PC via RF connectivity. The data was then post processed on the PC using various algorithms. The clinical study used five Parkinson disease subjects and 10 healthy subjects. Maximum pitch, Stride length, Minimum pitch, stride time and stance percentage were found using the data analysis performed. The data was validating against Massachusetts General Hospital bio motion laboratory's dataset.

Chen *et al.* [21] introduced a system for detection of abnormal gait using accelerometer gyroscope in the form of inertial measurement unit IMU, in addition to force sensing resistors (FSR) plus one bend sensor. The data was acquired at a frequency rate of 50 Hz and transmitted to the PC using RF communication. Post-processing predicted the abnormal gait in human beings and classified them to detect the pattern of toe in, toe out, heel walking, normal gait and other such gait abnormalities. Principal component analysis and support vector machines were few of the types of the algorithms used to classify the activities. There was no validation against a gold standard comparison.

Leunkeu *et al.*'s [22] research compared the patterns of pressures on the plantar surface during walking between able-bodied or and children with cerebral palsy using parotech plantar pressure insoles. The frequency at which the data acquired was 150 Hz. The data was logged in SD card and post processed on PC. The experiment was performed on 10 normal children and 10 children with cerebral palsy. The parameters calculated were double support time, ground contact time, step frequency, stride length and step duration. No comparison against a gold standard device was made.

Rampp *et al.*'s [23] research calculated spatial and temporal gait parameters with the help of an accelerometer and gyroscope which were embedded below the ankle joint on each foot. The frequency rate at which data got acquired was 102.4 Hz. The data was logged using Shimmer 2R, a commercially available product and post processed on PC. The study was validated with market product GAITrite. The experiment was conducted on a total of 116

patients. The computed parameters included swing time, stance time, stride time and stride length.

Mariani *et al.*'s [24] research included the motor symptoms characterization for Parkinson disease using accelerometer and gyroscope in which the data was acquired at a frequency rate of 200 Hz and it was logged into onto an SD card. Gait parameters were computed on the PC using post-processing techniques. The experiment was carried on 10 healthy subjects and 10 Parkinson disease patients. The computed parameters included stride length, path length, stride velocity and turning angle. The data was validated against the optical system by Vicon Motion Systems.

Kong *et al.* [25] measured the ground contact forces to detect the phases of human gait using a custom made sensor to detect the changes in air pressure. Fuzzy Logic was used to classify the different phases of gait. The data was acquired at a sampling frequency of 200 Hz and transmitted using National Instruments Compact Rio data logger. The abnormalities were indicated after the post processing on the data acquired. There was no gold standard comparison made in the study.

González *et al.* [26] used a fuzzy logic based algorithm to classify each gait phases using force sensitive resistors and accelerometers. The data acquisition frequency was 50 Hz and the data was transmitted to the PC via Bluetooth connection wirelessly. The data was post processed on PC and real time monitoring was being done on a smartphone. The device was tested on six of healthy subjects using a fuzzy logic based inference algorithm. The device has not been cross verified against a gold standard comparison.

Crea *et al.* [27] used an optoelectronics sensing based pressure-sensitive insole in which the data was acquired at a frequency rate of 18.75 Hz. It was transmitted to the PC via Bluetooth connection wirelessly. The data could be visualized on LabVIEW in the real-time fashion. The data had been validated on two healthy subjects. The parameters calculated were swing duration, double support time, step cadence and stance percentage. The device was validated against AMTi force plate as a gold standard comparison parameter.

Ferrari *et al.* [28] used Kalman filter to identify gait events complying with pathological gait patterns. 3 Axis accelerometer and 3 Axis gyroscope as inertial sensors, acquiring the data at a frequency rate of 200 Hz. The data was sent using Bluetooth to the smartphone in the form of a mobile app to process the data in real time. Post-processing of the data was also be done on the PC. The experiment was carried out on 16 Parkinson Disease subjects and 12 healthy

subjects. The parameters calculated were stride time, stride length, step length and stride velocity. The device was validated against GAITRite as a gold standard comparison.

Lin *et al.* [29] used an array of sensors on a textile fabric based on the properties of softness, lightness and high sensitivity with a long service life. The data was acquired at a frequency rate of 100 Hz and it wirelessly transmitted to PC and smartphone using Bluetooth. The data could be visualized in real time. The parameters displayed were centre of pressure, speed of the centre of pressure and mean pressure. The device was validated against a standard force plate.

Sazonov *et al.* [30] studied the temporal gait parameters of patients with rehabilitation after stroke to assess the ability of lower extremity utilization. The footwear had an accelerometer and force sensitive resistors embedded in it. The data was required at a frequency rate of 25 Hz and transmitted to a smartphone via Bluetooth. Gait parameters were calculated on a PC after acquiring the data. The study was conducted on 7 stroke patients and 16 healthy subjects. The parameters calculated were cycle time, swing percentage, stance percentage, double support percentage, and single support percentage and step time. The device was validated against GAITRite as a gold standard comparison.

Kawsar *et al.* [31] used 8 pressure sensors embedded in fabric to classify different activities in patients. In addition 3 Axis accelerometer and gyroscope inside the smartphone were also used. The data was acquired at a frequency rate of 37 Hz and transmitted to smartphone via Bluetooth wirelessly. The activities were classified into four cases which were sitting, standing, running and walking. The data could be visualised in real time on Android Smartphone and there was no gold standard comparison made.

Hegde *et al.* [32] designed insole based embedded wearable sensor which could be used for generic shoes thereby reduced the need for shoe modification. The insole had Force Sensitive Resistors, 3-axis accelerometers, and gyroscope. The data acquiring rate could be set to a range from 25 Hz to 75 Hz and the data could be transmitted to smartphone via Bluetooth. The data acquired was post processed and classified for activity recognition using multinomial logistic discrimination. The activities that were classified were cycling, sitting, walking and standing with real time display on a smartphone. The device was validated on five healthy subjects with no comparison to a gold standard device.

Donovan *et al.* [33] designed an auditory feedback device so that the plantar pressure on the lateral area of the foot can be reduced. The data was acquired using Pedar-X planter

pressure measurement system and EMG at a frequency rate of 100 Hz. The system was not wireless for transmission rather the data was logged via wired interface. The data was computed in a real time fashion with active generation of biofeedback. The device was validated on 9 subjects with chronic ankle instability.

Chapter 3 : MATERIALS AND METHODS

3.1 Premise

In the present research work five subjects' data was taken and each subject was asked to walk with the customised insoles for three different terrain/path lengths 12 meter, 16 meter and 20 meter, respectively. The data was recorded on all the three trials for all the subjects for the post processing to be done. The path chosen was a university corridor and markers were placed on each start point and stop point as shown in Figure 3.1. The subject was asked to start the trial on the given command and to stop once the marker for that particular trial reaches.



Figure 3.1: Distance/Path Measurement and Marker Placement:

During the experiment the data was collected continuously without any break to maintain the integrity of the dataset. All the trials were taken in a single event only, in other words the subject was asked for three trials in a single session. Once the foot print was recorded in a sand box, the sensors were placed in the respective maximum pressure locations on the insole. Then the subject was asked to wear the sandals with the insole embedded in-between the foot and sandal.

3.2 Experimental Protocol

- The subject was made to stand in the sandbox barefoot three times, in order to remove any error due to wrong placement of foot in the first place.
- The sensor locations were marked on the footprint in the sandbox using a needle by visual observation.
- Necessary adjustments were made to the sensor locations on both the insoles for accurate recording of data while experimentation.
- The subject was made to wear sandals with insole system in between them with or without socks.
- The subject was asked to get comfortable with the new device, by taking a walk at a normal pace till he/she feels comfortable physically as well as psychologically.
- Experiment started after the subject was asked to walk normally in walkway/ corridor from and to a specifically marked point.
- Finally, subject was asked to carefully remove the sandals for the next subject.

3.3 Precautions

- The subject was made to get comfortable before the trials, so that there is no hesitation in the mind of the subject, due to which the gait of the subject should not alter.
- Five minute rest to the subject was given in between the tests, so that the subject may not get fatigued and the sensors get appropriate time to reset.
- After the device was worn each, every sensor on the insole was tested. The subject was asked to deliberately press the sensors on each location and the response was checked at the receiver end i.e. at PC to ensure that all sensors give the response.
- The subject was made aware of the markers, i.e., each path length.

3.4 Communication Protocol Trials

3.4.1 Communication using WiFi module

The communication between the feet modules and the computer was done using a NodeMCU module. It has integrated WiFi module and a MCU with analog and digital pins. The data from each foot module was proposed to be transmitted to web or an IP address to make the device as an IOT device. The IP address was local IP address, created by the NodeMCU module to stream data online Figure 3.2. The next step was to downstream the data into MATLAB for further processing. There were few hitches, which led to dropping this idea for communication.

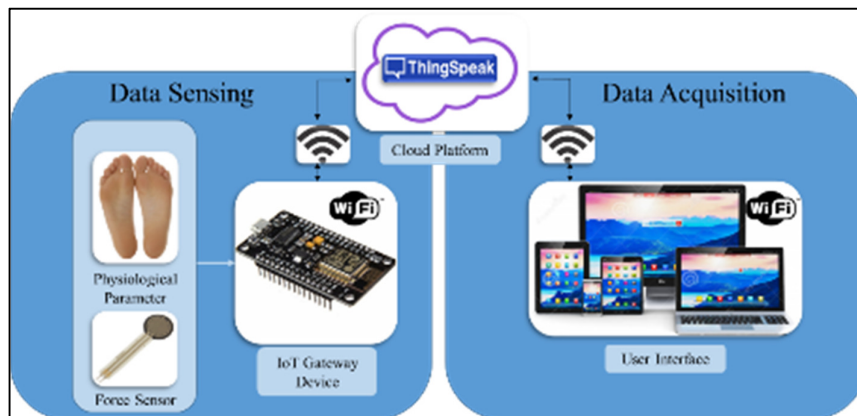


Figure 3.2: Communication using WiFi Module

Through the softwares, one can connect to the internet or an IP address and stream data. In MATLAB, the Simulink has various blocks for streaming data and it can be done via command line also. Firstly, the up-streaming of data from NodeMCU was itself a major task. The data being sent on web was reloading the page repeatedly, thereby destabilising the established connection and breaking the connection with MATLAB. The solution to above problem was proposed to create a webpage, use java script and AJAX to update the data field, live. But the solution involved too much of scripting languages, which might end up taking all of the time thereby defeating the purpose of the research work. The target device will not be used very far away from the host device and the application was time critical, for which the WiFi technology was not suitable, due to the unstable nature of the protocol. The benefits of including WiFi protocol were, the data can be transmitted all over the world and can be seen doctors anywhere for clinical treatment. This step can also be performed once the data was acquired onto the PC via any other method of acquisition.

3.4.2 Communication using Bluetooth module

The other solution was to use Bluetooth for the communication. But, multiple data streaming devices i.e. from both the feet posed complications in the data exchange between each other and the master/PC. The Bluetooth protocol works on one to one communication basis. Using two Bluetooth devices was not viable, as there was a high chance of data loss while trying to connect with the master module. Bluetooth communication itself draws very heavy current unless, BLE is used. This protocol was not a good fit for the application in hand due to the multi slave nature of the research work.

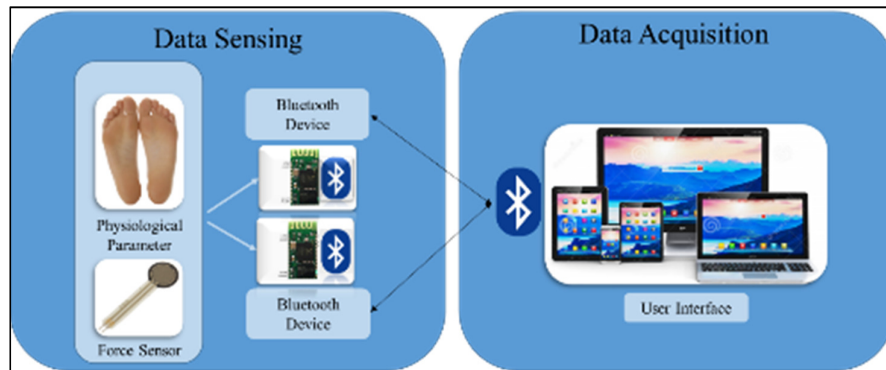


Figure 3.3: Communication using Bluetooth Module

The Bluetooth protocol was particularly beneficial when the data was transmitted to the mobile phone for display and personalisation. For clinical application, such as in this case, the communication was made to the PC for research analysis as shown in Figure 3.3. MATLAB has inbuilt support for Bluetooth communication in the form of blocks. This feature might be added in the future versions of the device to provide in app facility of acquisition and representation. Packet size detection and variability was a major issue to encounter in communication protocol. Here, the detection represents that the cloud / master should automatically detect the data bits/bytes being sent by the slave and decode the message encoded in it correctly.

3.4.3 Communication using RF module

The third way out which was explored by using RF communication and for this methodology nRF24101 RF module was chosen. This chip works on 2.4GHz ISM band frequency. Serial Peripheral Interface (SPI) communication protocol was used. The data from the pressure was acquired by the (Force Sensitive Resistance) FSR sensors and relayed to the Microcontroller Unit (MCU).

The RF module connected to the MCU collected the data and transmitted it to the master module connected with the PC. The MCU and RF module were fused together to act as one module and two of them to act as slaves (one for each foot). The other one acts as a master module tethered with PC for data logging/acquisition. Each slave module relayed the acquired data one packet at a time.

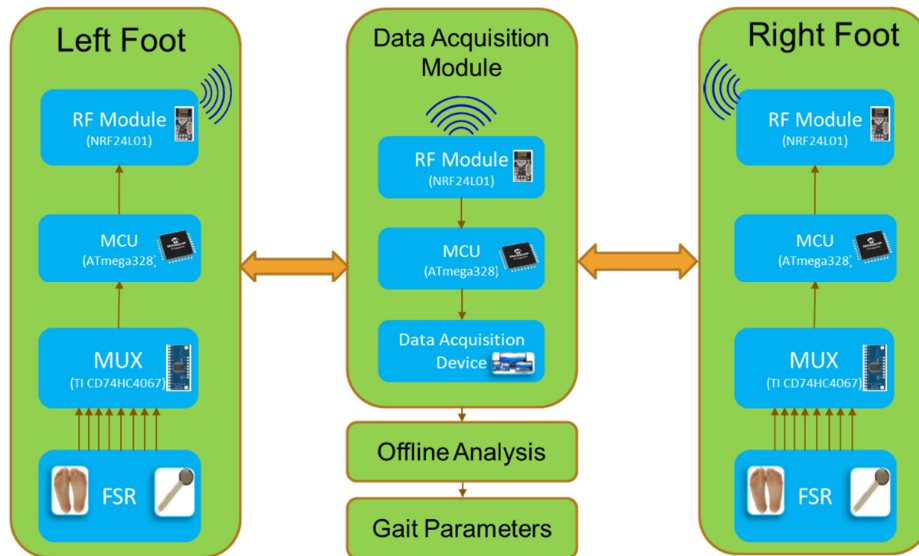


Figure 3.4: Basic Block Diagram

The slave modules were programmed to transmit eight packets of data corresponding to eight sensors acquiring data from a foot as shown in Figure 3.4. The data from the sensors was acquired in a particular sequence, starting from the heel area, to the outer midfoot area, to the forefoot area and then then to the inner midfoot area (arched area). After the data from one slave was transmitted to the master module, the second slave was asked for the data and it transmitted the data in a similar fashion.

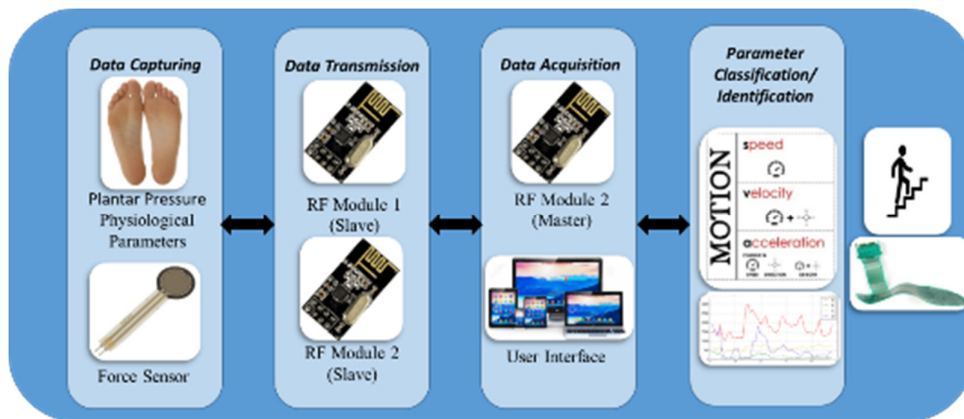


Figure 3.5: Communication using RF Module

This procedure was performed continuously to acquire data. In technical terms polling was done between the two slaves and the master for data acquisition. The data received by the master was continuously logged in an excel sheet.

The slaves only responded with the data when they were asked for the data. Every time the data was received by the slave, who sent an acknowledgement to the master informing the particular slave pinged in. The data transfer rate between master and slave modules was user defined as 250kbps. The dataset acquired from a particular subject was then analysed in MATLAB to find out different parameters. The complete cycle can be visualised in Figure 3.5. Variation in centre of pressure (COP) of the feet, minimum pitch, maximum pitch, stride length, stance timing, cycle timing, swing percentage, single support percentage, double support percentage, step duration, velocity and step frequency were the parameters that were calculated.

The data acquired from each sensor was compiled and plotted on a single graph which depicted the frequency of activation. Here, eight sensors were used to send eight analog signals. Therefore, eight input channels were used to the MCU. Due to lack of multitudinous analog channels, the sensor outputs were multiplexed using CD74HC4067 multiplexer.

3.5 Data Communication Module Construction

3.5.1 CD74HC4067

Similar to a rotary switch this breakout board route the acquired data from one of the 16 pins to output via com pin. The device was extremely convenient for digital/analog, demultiplexer/multiplexer up to 16 channels. The IC used in this break out board was CD74HC4067 as shown in Figure 3.6.

The board was used to control analog signal. It can also be used for digital signals. By connection of four digital outputs from a microcontroller to the address select pins (S0-S3) of the board was controlled.

Binary address of the required channel was sent to the chip select pins, thus allowed to connect upto 16 sensors with the system. TTL serial data was be streamed to and from multiple devices as it works with digital signals as well [34].

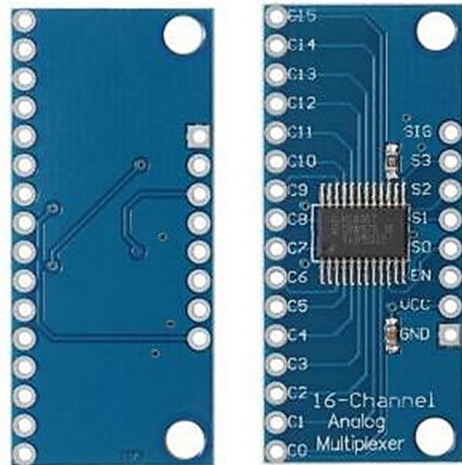


Figure 3.6: Analog Multiplexer

It supports break-before-make type switching to prevent damage to devices and prevent crosstalk. It has low off leakage and low on resistance and the internal switches are bidirectional. The board also has “enable” pin, and when driven high, it will disconnect the common pin (all switches “off”).

3.5.2 Arduino Nano

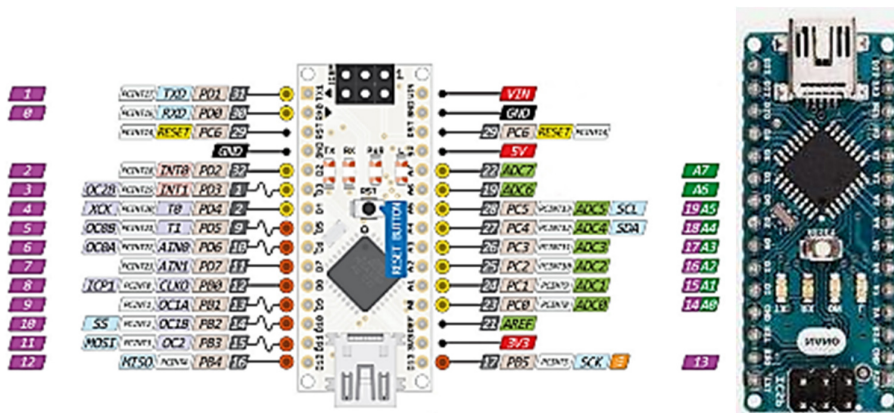


Figure 3.7: Arduino Nano

This MCU is a complete, tiny and breadboard compatible board which runs on the ATmega328 (Arduino Nano 3.0) or ATmega168 (Arduino Nano 2.0) microcontrollers. The operating voltage is 5 V and the input voltage recommended, ranges from 6 to 20 V. It has 8 analog pins and 14 digital input/output pins as shown in Figure 3.7. The current sinking or sourcing capacity is around 40 mA. The SRAM in ATmega168 is 1KB or 2KB in ATmega328 and the Flash memory is 16KB in ATmega168 and 32KB in ATmega328 of which bootloader uses 2KB. It supports crystal frequency of 16 KHz. Each of the analog pin provide 10 bits of resolution (i.e. 1024 different values). The default potential difference is

5V, although it is possible to change the upper end of their range using the analog Reference () function[35].

The ATmega328 and ATmega168 provide UART serial communication, available on digital pins 1 (TX) and 0 (RX). An FTDI FT232RL on the board helps with serial communication via USB and the FTDI drivers provide a com port to software on the PC. The Arduino IDE includes a serial monitor which allowing textual data to be sent to and from the MCU. The TX and RX LEDs on the board will blink when data is being transmitted via the FTDI chip and USB connection to the computer. The ATmega168 and ATmega328 also support SPI and I2C communication.

3.5.3 Interlink force sensitive resistor

Force Sensing Resistors (FSR) is a resistive device its value decreases with an increase in the force applied on the active surface. The sensor can be seen in Figure 3.9. Its force sensitivity is adjusted for use in human touch leading to control of electronic devices. FSRs are not recommended for precision measurements. The force vs. resistance characteristics shown in Figure 3.8 provides the typical response behaviour in a log-log format. FSR response follows an inverse power-law characteristic (roughly $1/R$).

Figure 3.8, shows that at low force end, it responds like a switch. This break force or turn-on threshold swings the resistance from greater than $100\text{ k}\Omega$ to about $10\text{ k}\Omega$. It is determined by the substrate, overlay, flexibility, size, actuator shape and spacer-adhesive thickness. At high force end in the characteristics, the deviation in sensor response from the power-law behavior was quite distinguishable, and it saturates to a point where an increase in force yield little or no decrease in resistance. Under these conditions of Figure 3.8, this saturation force is beyond 10 kg .

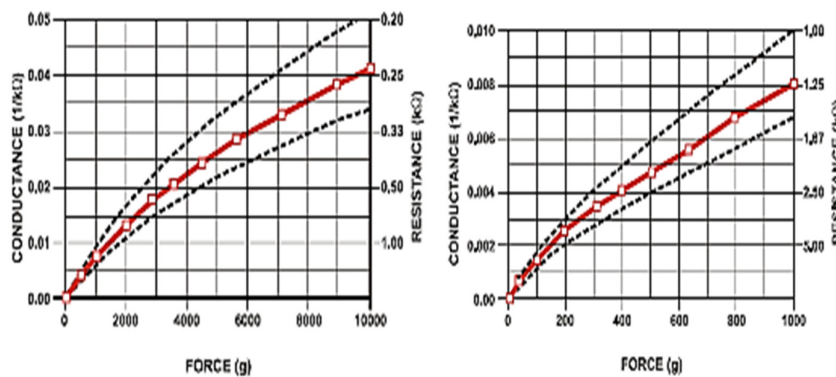


Figure 3.8: FSR Response Curves

Forces higher than the saturation force can be measured by scattering the force over a large area [36]. The overall pressure is then kept below the saturation point in addition to maintaining the dynamic response. In Figure 3.8, the conductance is plotted vs. force (the inverse of resistance: $1/r$). This format allows interpretation on a linear scale. For reference, the corresponding resistance values are also included on the right vertical axis. Figure 3.8 also includes a typical part to part repeatability envelope. Maximum accuracy is determined by error band of any general force measurement. The spread or width of the band is dependent on the repeatability of actuating and measuring system, in addition to the repeatability tolerance held by industry during FSR production. Typically, the part-to-part repeatability tolerance ranges from 15% to 25% of an established nominal resistance. Figure 3.8 highlights 0-1 kg range of the conductance force characteristic and it correspond to resistance values included for reference. This range is common to human interface applications. The conductance response in this range is fairly linear so, the force resolution will be uniform and data interpretation will be simplified. In most human touch control applications this error is insignificant, as human touch is fairly inaccurate. Human factors studies have shown that in this force range repeatability errors of less than 50% are difficult to discern by touch alone [36].



Figure 3.9: FSR Sensor

3.5.4 Nordic nRF24L01+

The nRF24L01 is an ultra-low power integrated 2Mbps RF transceiver IC and works in the 2.4GHz ISM (Industrial, Scientific and Medical) band. It has peak RX/TX currents lower than 14mA and a 1.9 to 3.6V supply range with integrated voltage regulator. It can be operated and configured through a serial peripheral interface (SPI). It supports dynamic payload ranging from 1 to 32 bytes with automatic packet handling and 6 data pipe

multiceiver for 1:6 networks. Features include 26uA standby mode and 900nA power down mode. The device can be visualise in Figure 3.10.

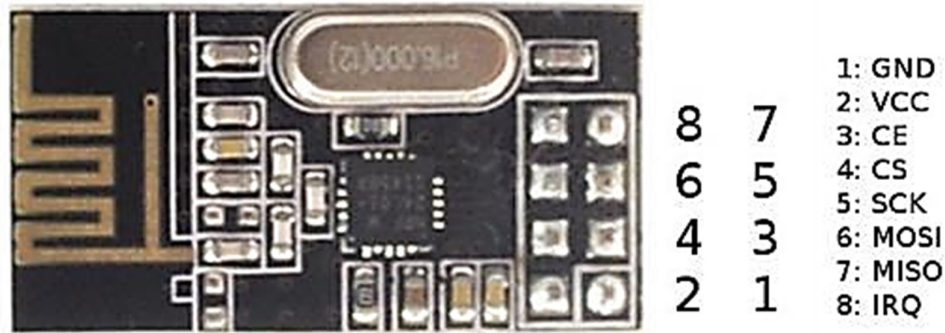


Figure 3.10: NRF24L01 RF Module

Internal voltage regulators ensure that the device has high Power Supply Rejection Ratio (PSRR) and wider power supply range. The application areas include wireless PC peripherals, game controllers, sports watches and sensors, consumer electronics, home and commercial automation and active RFID *etc.* [37].

3.6 Parameters Calculated

Centre of Pressure (CoP)

The mathematical expressions for CoP are described in equations discussed below.

$$M_{i|x} = P_i \times Y_i \quad (1)$$

$$M_{i|y} = P_i \times X_i \quad (2)$$

$$X_{CoP} = \frac{\sum_{i=1}^n M_{i|y}}{\sum_{i=1}^n P_i} \quad (3)$$

$$Y_{CoP} = \frac{\sum_{i=1}^n M_{i|x}}{\sum_{i=1}^n P_i} \quad (4)$$

In the above equations $M_{i|x}$ and $M_{i|y}$ are moments of pressure P_i about X and Y respectively. X_i and Y_i being coordinates of each sensor location i, with respect to foot coordinate system of insole and n is no. of sensors, where X_{CoP} and Y_{CoP} are the coordinates of Centre of Pressure. Also, called sum of all the Ground Reaction Forces (GRF).

The parameters in addition to CoP are described in Table 3.1.

Table 3.1: Parameters used

Stride Length	HS of one foot to the next HS of the same foot was calculated by dividing the walk distance by the stride count for each foot respectively.
Step Length	It was calculated by observing the length of HS of one foot to HS of the other foot.
No. of Steps Average Velocity	Average velocity was calculated by division of total walk distance (trial dependent) and total time.
HS Event	The timing event when the heel strikes ground every time a step was taken. It is important in development of ankle prosthetics.
Toe Off (TO) Event.	The timing event when a step was complete and swing phase starts.
Stance %	It was the value which describes the percentage of time the any part of the foot touched ground or the time between the HS and the next TO.
Swing %	It was the value which describes the percentage of time a particular foot was in air or the time between a TO and the next HS.
Single Support %	% of total time when only single foot was touching the ground.
Double Support %	% of total time when both the feet were touching the ground.
Centre of Pressure (CoP)	Central point where all the forces acting on the different points on the foot could be summed to.
Total Time Taken	Total time taken was described by the dataset itself as the each data point was saved with a timestamp when saved, so the total time period was the timestamp of the last sensor reading.
No. of strides	Number of strides was the number which describes the total number of strides taken by the subject per foot to complete the trial path. It could be different or same for each foot.

3.7 Sensors Localization

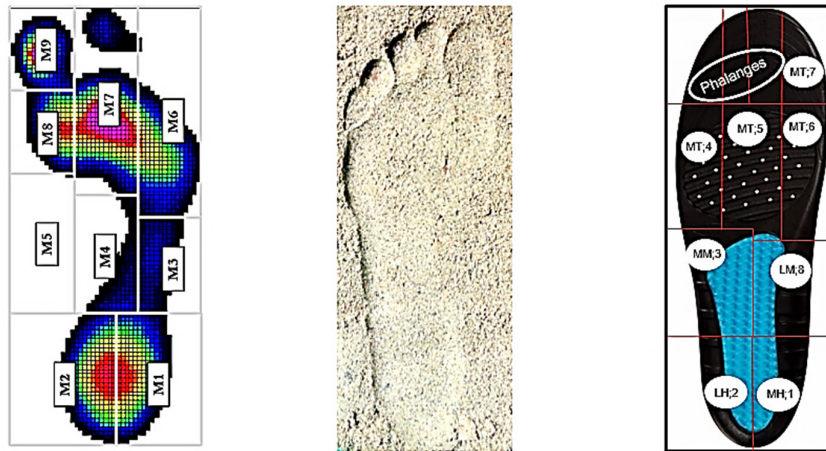


Figure 3.11: Sensor Locations

The sensor locations were followed from the pressure points found from the sand pressure protocol as can be seen in Figure 3.11.

3.8 Complete Hardware Device

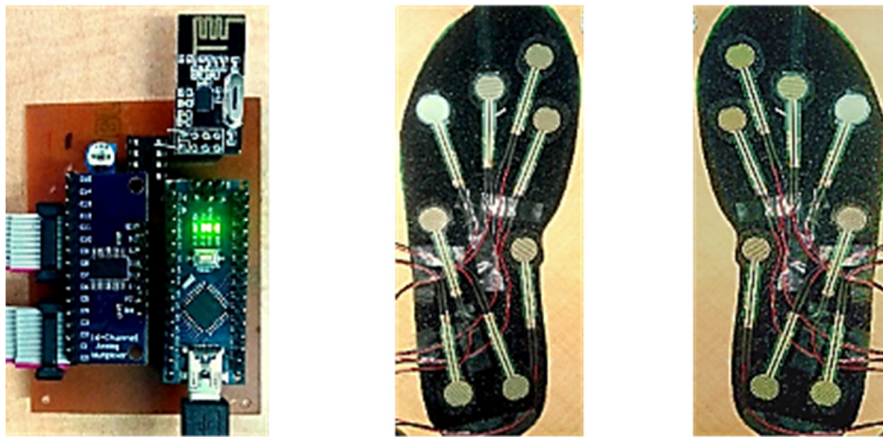


Figure 3.12: Complete Device with Insoles

The data transmission module with insoles can be seen in Figure 3.12. Both the insoles had their own data transmission modules to transmit the acquired data and the data was transmitted to the master module (connected to the PC/User Interface) in a polling fashion. Figure 3.14 shows the generic placement of the sensors on the left foot and sensors were placed on the right insole as well.

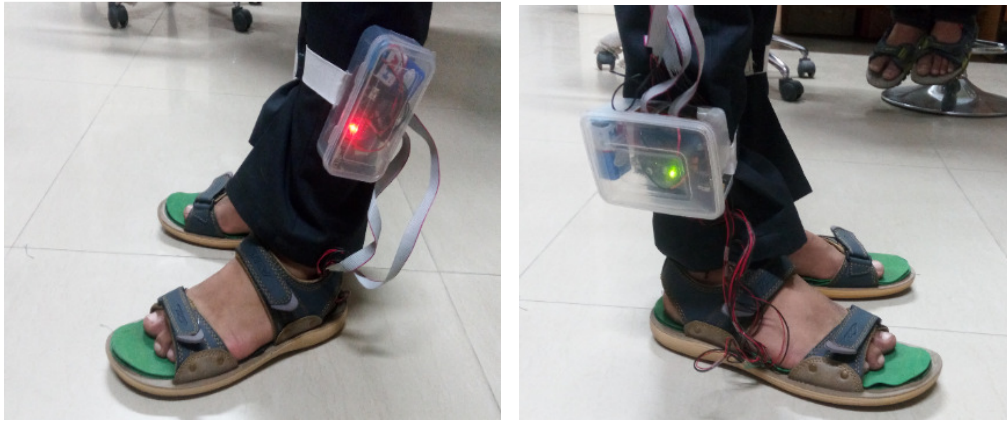


Figure 3.13: Subject Wearing the Insoles in Left (Red LED) and Right (Green LED) foot

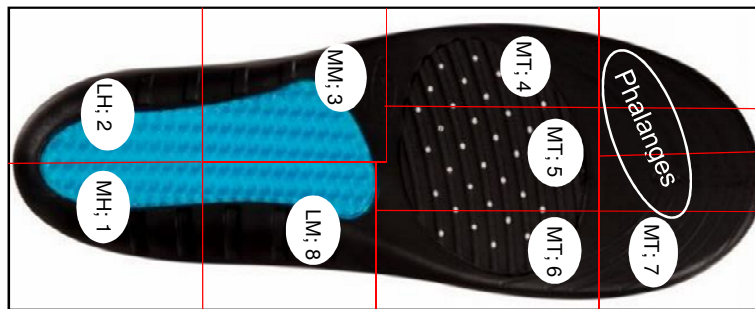


Figure 3.14: Generic Sensor Placement on the Left Insole

The master module asked for data to both the modules in a loop. If any of the slave modules failed to transmit data due to any reason, which included environmental disturbance *etc.*, the master module stopped to acquire data. It waited for the packet to be received and then moved forward to collect data from other sensor. Figure 3.13 show the subject wearing the complete device before experimentation.

Chapter 4 : RESULTS AND DISCUSSIONS

4.1 Outcomes

The data collected was processed in MATLAB and various parameters were calculated which are mentioned in Tables 1, 2 and 3.

Table 4.1: Parameter Table for 12 Meter Path Trials

Subject 1 – 12 Meter	Trial 1		Trial 2		Trial 3	
	Left	Right	Left	Right	Left	Right
Stride Length (m)	1	1.09	1.09	1.2	1.09	1.2
Average Velocity (m/sec)	0.67	0.67	0.70	0.71	0.75	0.74
Total Time Taken (sec)	17.71	17.76	16.95	16.85	15.98	16.01
No. of Strides taken	12	11	11	10	11	10
Swing %	57.52	64.16	55.77	58.20	56.35	61.07
Stance %	42.47	35.83	44.22	41.79	43.64	38.92

Table 4.2: Parameter Table for 16 Meter Path Trials

Subject 1 – 16 Meter	Trial 1		Trial 2		Trial 3	
	Left	Right	Left	Right	Left	Right
Stride Length (m)	1.14	1.14	1.23	1.23	1.14	1.33
Average Velocity (m/sec)	0.78	0.78	0.84	0.83	0.82	0.82
Total Time Taken (sec)	20.32	20.32	19.04	19.07	19.42	19.34
No. of strides taken	14	14	13	13	14	12
Swing %	60.36	61.25	59.55	62.07	60.35	60.29
Stance %	39.63	38.74	40.44	37.92	39.64	39.70

Table 4.3: Parameter Table for 20 Meter Path Trials

Subject 1 – 20 Meter	Trial 1		Trial 2		Trial 3	
	Left	Right	Left	Right	Left	Right
Stride Length (m)	1.25	1.33	1.33	1.25	1.33	1.33
Average Velocity (m/sec)	0.95	0.95	0.90	0.90	0.93	0.93
Total Time Taken (sec)	20.85	20.85	22.00	22.03	21.39	21.34
No. of strides taken	16	15	15	16	15	15
Swing %	57.50	61.55	54.95	53.46	57.51	52.42
Stance %	42.49	38.44	45.04	46.53	42.48	45.57

Table 4.1, 4.2, and 4.3 data for various markers shows that the stance and swing percentages, that the swing percentages of the left foot are lower than, the swing percentages of right foot and stance percentages for left foot are greater than the stance percentages of right foot. This means, the subject spends more time with the left foot on the ground than right foot alternatively, the subject spends more time with the right foot in air that left foot. It is also clearly visible from the tables that the number of strides increases as the distance to cover increase. Similarly, the linear relationship of time taken can be verified with quantified numerics.

Figure 4.5 and Figure 4.6 indicate that the trajectory of right foot of the subject is relatively smaller than the CoP trajectory of the left foot. This fact is verified quantitatively, by the numerics form the Table 4.1, 4.2, and 4.3.

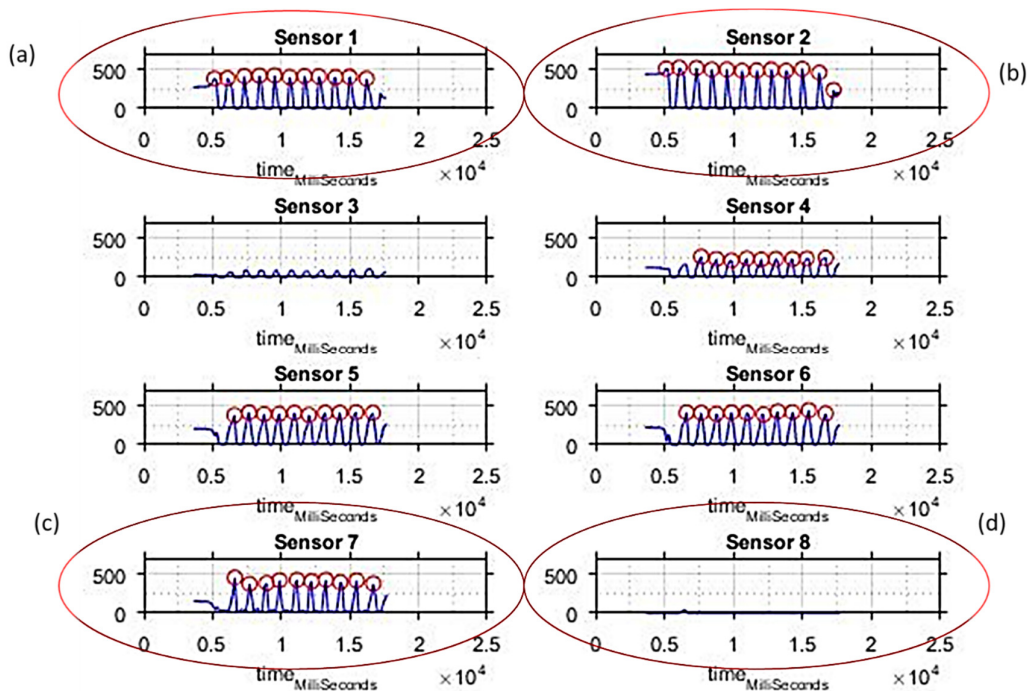


Figure 4.1: Trial Data for Left Foot

Figure 4.1 (a) and (b) correspond to the heel sensors and have equal number of peaks in both the plots depict that the subject lands on the heel in a straight fashion and thus is not suffering from overpronation or oversupination. The timing of the peaks on both the sensor verifies the claim. The peaks also depict an important parameter in physiological terminology known as “HS Event”, this event is crucial in development of intelligent prosthetics. Another important parameter is, the “TO Event” shown by Figure 4.1 (c), this event is crucial in the development of smart lower limb and ankle prosthetics. Figure 4.1(d)

i.e., 8th sensor shows the behavior of the sensor placed beneath the left midfoot region on the right foot and the right midfoot region on the left foot.

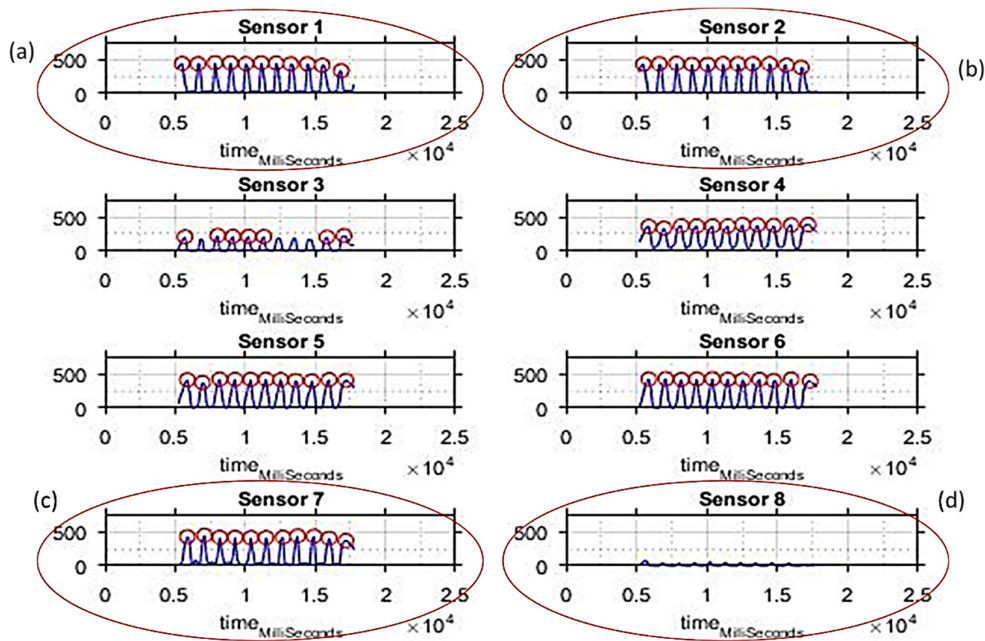


Figure 4.2: Trial Data for Right Foot

This sensor was placed to diagnose the medical condition of “Flat Foot” and the absence of any peak in both the figures show that the subject was healthy. The sensors 4, 5 and 6 help in the detection of a medical condition called lateral whip and medial whip. The whip conditions are calculated in association with TO sensor i.e. sensor 7. These results have been published in [38].

Figure 4.1 and Figure 4.2 correspond to each sensor placed in the insole at the designated location. Each of the sensors placed had a designated purpose or gave information about a particular physiological parameter. The trajectory of the centre of pressure for different trials are shown in Figure 4.3, i.e., for 12m, 16m and 20m, one for each trial for a particular path length. The blue lines depict the trajectory for individual strides and the red line depicts the average trajectory followed by the CoP of the foot. In each trial, visually it can be easily seen that all the individual trajectories are similar if not the same or follow the same pattern which shows that the first the device is consistent in its measurement and secondly the subject is healthy as it is not varying the gait trajectory.

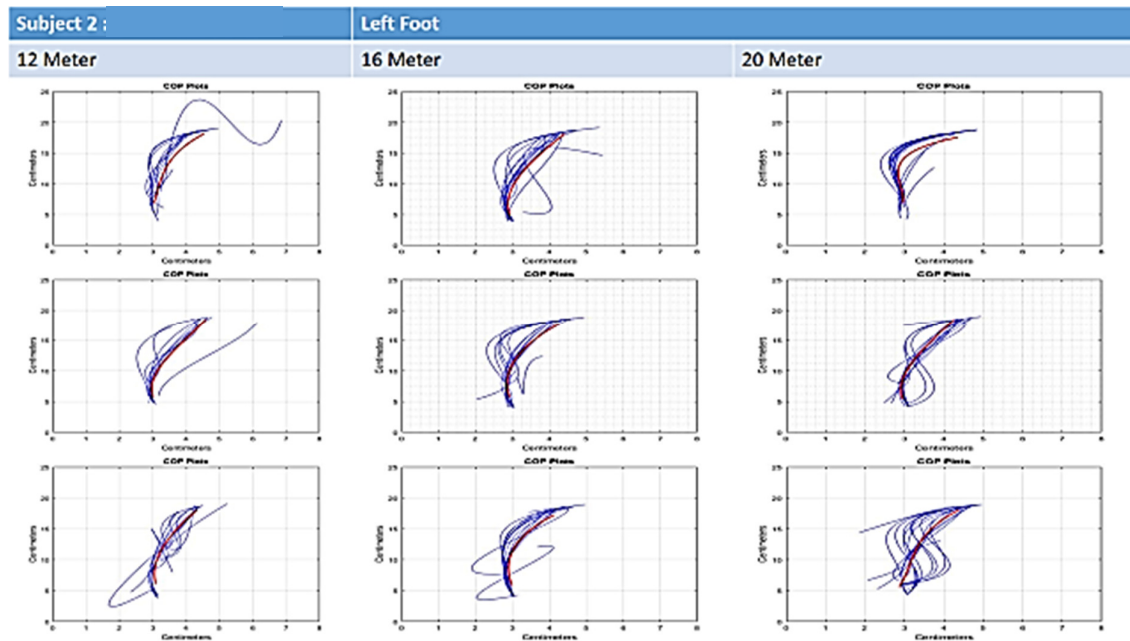


Figure 4.3: Centre of Pressure Plots for Left Foot for Subject 2

Similarly, it can be seen in the Figure 4.4 that the trajectory followed by the right foot is consistent and the device is highly repeatable in addition to informing that the subject is healthy.

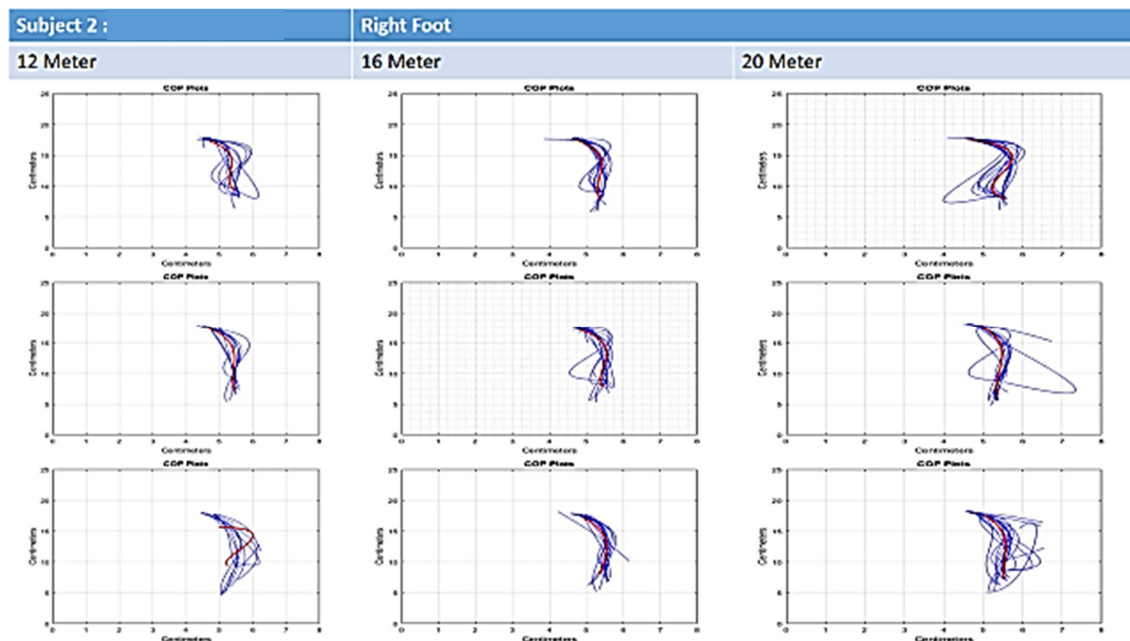


Figure 4.4: Centre of Pressure Plots for Right Foot for Subject 2

The Figure 4.5 shows both the trajectories on a single image for each trial and the consistency can be easily verified. The combined plots for other subjects can be visualised in Annexure.

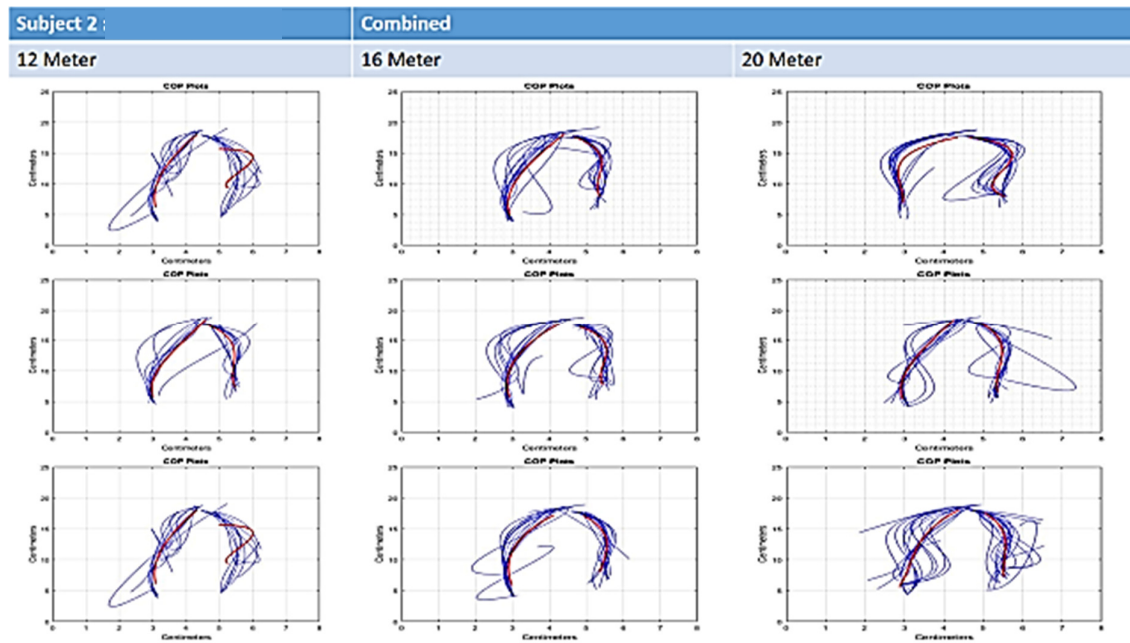


Figure 4.5: Centre of Pressure Plots for Both Feet for Subject 2

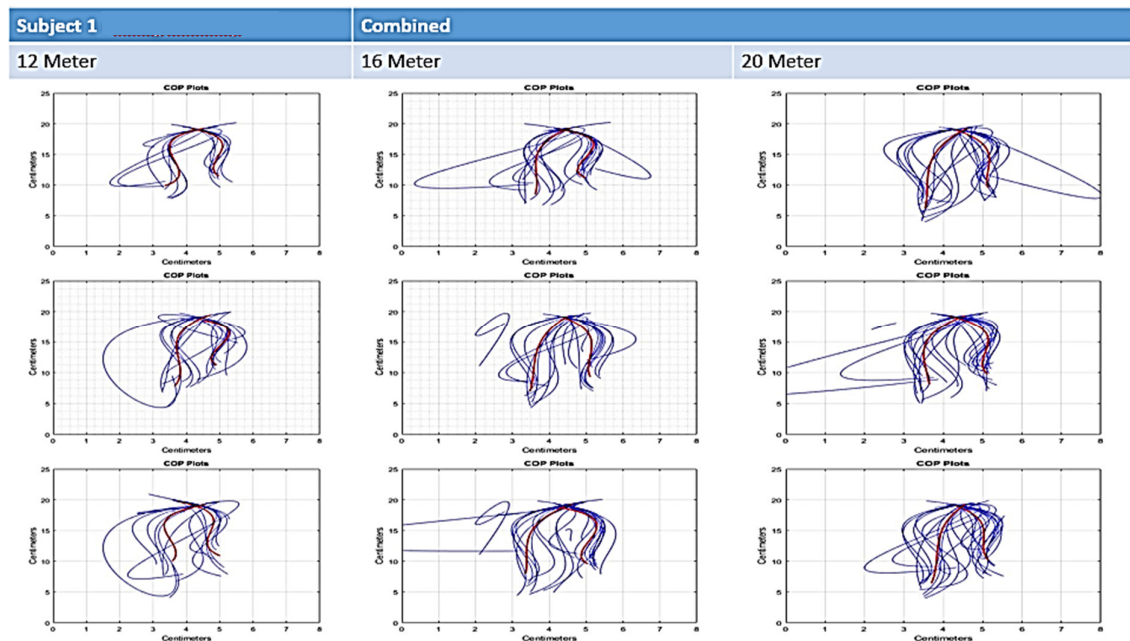


Figure 4.6: Centre of Pressure Plots for Both Feet for Subject 1

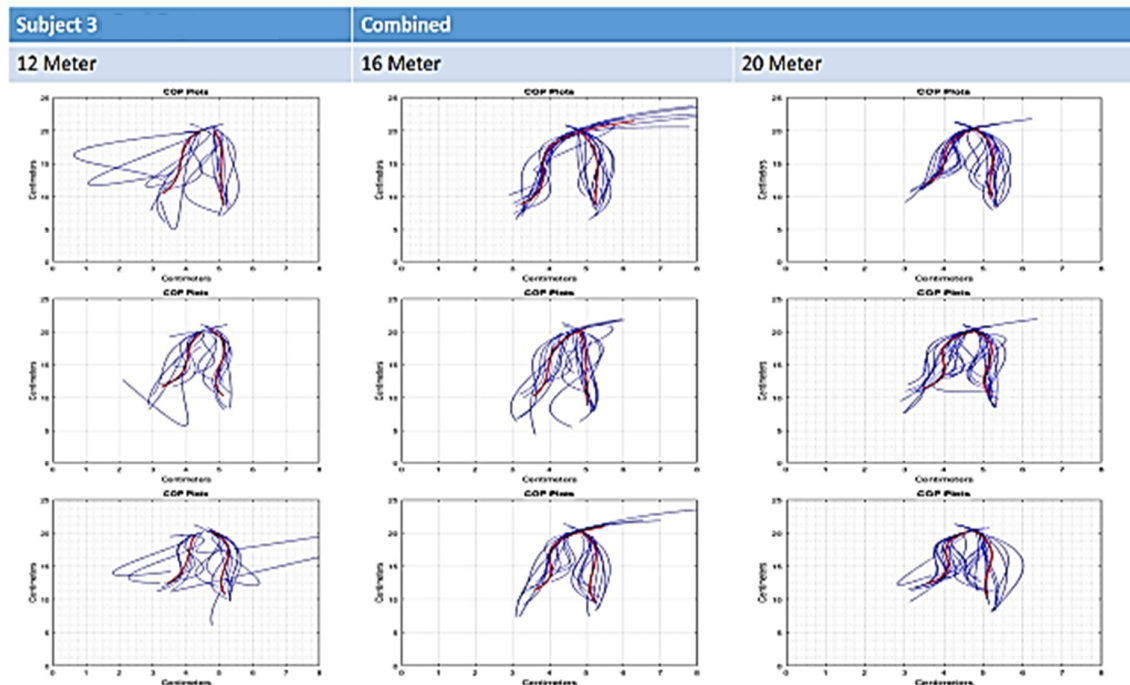


Figure 4.7: Centre of Pressure Plots for Both Feet for Subject 3

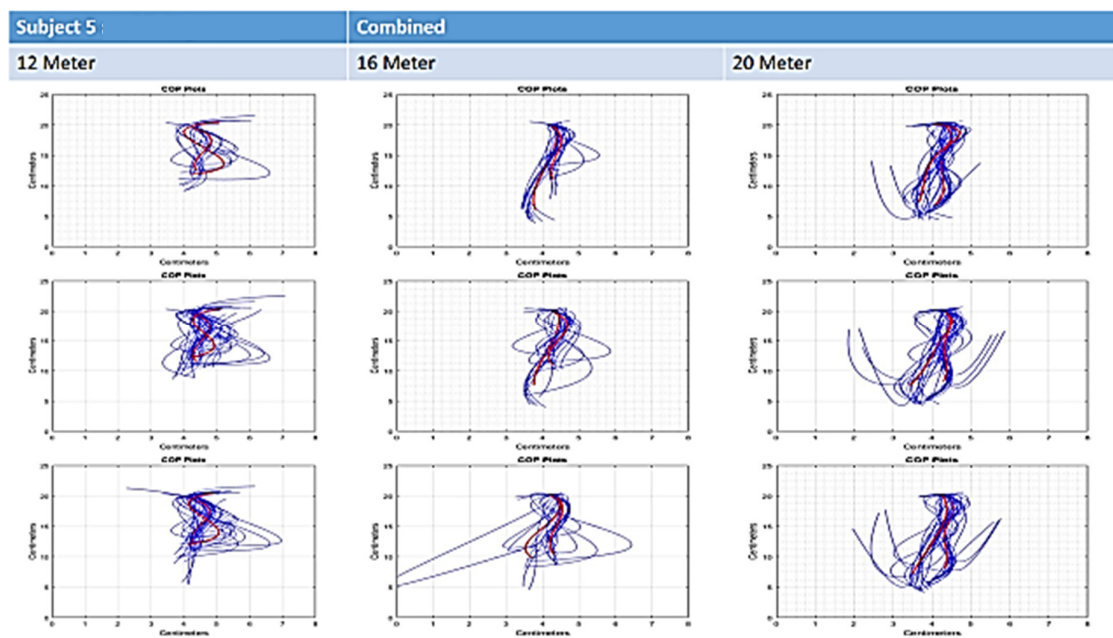


Figure 4.8: Centre of Pressure Plots for Both Feet for Subject 5

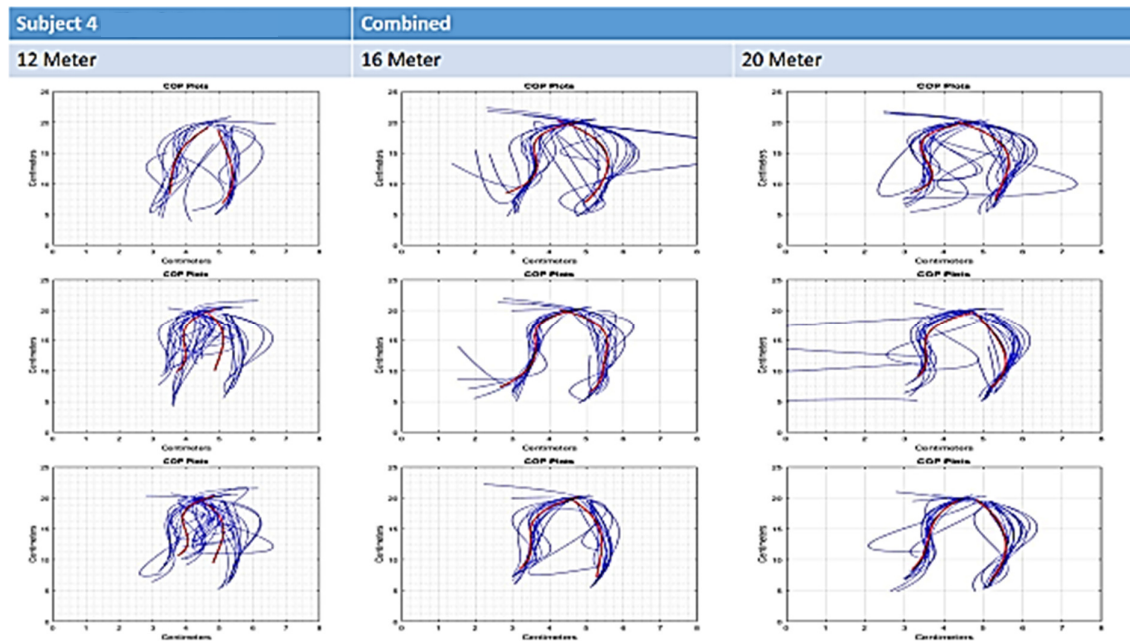


Figure 4.9: Centre of Pressure Plots for Both Feet for Subject 4

The consistency or the significance of the plot was verified by statistical method ANOVA. This statistical test was performed on individual trials to check whether the individual strides were consistent to each other. Results of p-value were more than 0.05, which shows that the data is similar and, there were no cases where the trajectory had deviated.

To verify the consistency of the gait in different trials i.e. to establish the fact, that the person's gait or the manner of walking remains consistent, irrespective of the distance, the ANOVA test was performed on the average right and left gait trajectories. The resulting p value was more than 0.05, which shows that there was consistency in the walking manner of the subject.

According to null hypothesis individual gait patterns in all the three trials should be different [39] i.e., the person walks differently. In the current research work ANOVA test was performed to verify the hypothesis. It is observed that it rejects the null hypothesis and the gait patterns were found similar statistically. Hence, by establishing the fact that the gait of a human being remains the same irrespective of the distance traversed or the repetition of trial keeping the distance same.

Chapter 5 : CONCLUSION AND FUTURE SCOPE

5.1 Conclusion

Gait characterization plays an important role in rehabilitation, lower limb prosthesis control, robotic control and preoperative disease quantification. In this study a low cost wireless pressures sensor based insole had been developed to capture change in foot pressures developed during locomotion. The location of sensors had been selected strategically as, each location possess unique information regarding gait cycle. A preliminary study was carried out to justify the efficacy of developed device by acquiring data of five subjects for three trials at different terrain/path lengths. The basic parameters like stride length, average velocity, centre of pressure *etc.* had been calculated successfully from acquired signal along with critical gait events. The promising performance of developed device justify its usability towards any application where, gait characterization plays an important role such as Parkinson's disease, cerebral palsy *etc.*

5.2 Future Scope

In the present research work, wired interface of the sensors with MCU pose a huge jungle of cables therefore, a certain amount of noise can interfere. The wires themselves can be replaced by a flex PCB, which will completely eliminate the need for wires. The sensors in the current insole are adjustable in nature, as they are adjusted according to the subject's foot size. The material used to fix the sensors to the sole is Velcro, which once sticks to itself is not easy to remove. In case of readjustment, the sensors had to be pulled out in some cases, which might lead to damage being done to the sensing area. Currently, the slave devices are able to successfully transmit the data in a radii of 20 meter, from the master module in open environment. This distance can be improved and the range can be extended, with the help of antennas. It will provide more freedom to the subject in terms of testing area. The size reduction of both the master and slave module's PCB can be done to make the device more compact. It will reduce the noise generated in the wired design. The sensors can be calibrated to achieve true value of the weight being applied on the force sensors. The calibration needs to be done with proper equipment with good sensitivity to achieve accuracy in the data. The results in the present device were calculated by post-processing of

data. This can be replaced by real time data calculation/processing and result calculation. A dedicated GUI based system can be developed to eliminate the need of manual intervention of entering specific details to proceed forward. A mobile application can be developed which displays the crucial information to the user in a friendly format. The device can be connected to the cloud and can be made a part of internet of things.

LIST OF PUBLICATIONS

- [1] A. Aggarwal, R. Gupta, and R. Agarwal, “Design and Development of Integrated Insole System for Gait Analysis,” in Eleventh International Conference on Contemporary Computing (IC3), IC3-2018, 2018, pp. 1–6. (Accepted)

REFERENCES

- [1] M. P. Murray, a. B. Drought, and R. C. Kory, "Walking Patterns of Normal Men," *J. Bone Jt. Surg.*, vol. 46, no. 2, pp. 335–360, 1964.
- [2] P. Taylor and J. D. Boyling, "A Review of: ' The Biomechanics and Motor Control of Human Gait ' By David A . Winter . (University of Waterloo Press , Waterloo , Canada , 1987 .) [pp . 72 .]," no. March 2015, 2010.
- [3] C. L. Vaughan, B. L. Davis, and J. C. O'Connor, *The Three-Dimensional and Cyclic Nature of Gait*. 1999.
- [4] H. Sadeghi, P. Allard, F. Prince, and H. Labelle, "Symmetry And Limb Dominance In Able-Bodied Gait: A review," *Gait Posture*, vol. 12, no. 1, pp. 34–45, 2000.
- [5] R. Gailey, "Review Of Secondary Physical Conditions Associated With Lower-Limb Amputation And Long-Term Prosthesis Use," *J. Rehabil. Res. Dev.*, vol. 45, no. 1, pp. 15–30, 2008.
- [6] R. Baker, "The history of gait analysis before the advent of modern computers," *Gait Posture*, vol. 26, no. 3, pp. 331–342, 2007.
- [7] J. J. Brunnekreef, C. J. T. Van Uden, S. Van Moorsel, and J. G. M. Kooloos, "Reliability of videotaped observational gait analysis in patients with orthopedic impairments," *BMC Musculoskelet. Disord.*, vol. 6, pp. 1–9, 2005.
- [8] A. M. Keenan and T. M. Bach, "Video assessment of rearfoot movements during walking: A reliability study," *Arch. Phys. Med. Rehabil.*, vol. 77, no. 7, pp. 651–655, 1996.
- [9] K. T. Manal and T. S. Buchanan, "Source : STANDARD HANDBOOK OF BIOMEDICAL ENGINEERING AND DESIGN CHAPTER 5 BIOMECHANICS OF HUMAN MOVEMENT," *Stand. Handb. Biomed. Eng. Des.*, pp. 1–26, 2004.
- [10] R. L. Linford, "Camera speeds for optoelectronic assessment of stride-timing characteristics in horses at the trot.," *American Journal of Veterinary Research*, vol. 55, no. 9. pp. 1189–1195, 1994.
- [11] D. M. Karantonis, M. R. Narayanan, M. Mathie, N. H. Lovell, and B. G. Celler, "Implementation of a Real-Time Human Movement Classifier Using a Triaxial Accelerometer for Ambulatory Monitoring," *IEEE Trans. Inf. Technol. Biomed.*, vol. 10, no. 1, pp. 156–167, 2006.
- [12] Q. Sun, Z. Zhou, J. Jiang, and D. Hu, "Gait cadence detection based on surface electromyography (sEMG) of lower limb muscles," *2014 Int. Conf. Multisens. Fusion Inf. Integr. Intell. Syst.*, pp. 1–4, 2014.
- [13] R. T. Lauer, B. T. Smith, and R. R. Betz, "Application of a neuro-fuzzy network for gait event detection using electromyography in the child with cerebral palsy," *IEEE Trans. Biomed. Eng.*, vol. 52, no. 9, pp. 1532–1540, 2005.

- [14] I. A. F. Stokes, S. M. Henry, and R. M. Single, "Surface EMG electrodes do not accurately record from lumbar multifidus muscles," *Clin. Biomech.*, vol. 18, no. 1, pp. 9–13, 2003.
- [15] F. Dierick, M. Penta, D. Renaut, and C. Detrembleur, "A force measuring treadmill in clinical gait analysis," *Gait Posture*, vol. 20, no. 3, pp. 299–303, 2004.
- [16] "Wearable Sensors - APDM Wearable Technologies." [Online]. Available: <https://www.apdm.com/wearable-sensors/>. [Accessed: 01-May-2018].
- [17] "pedar." [Online]. Available: <http://novel.de/novelcontent/pedar>. [Accessed: 01-May-2018].
- [18] J. J. Wertsch, J. G. Webster, and W. J. Tompkins, "A portable insole plantar pressure measurement system," *J. Rehabil. Res. Dev.*, vol. 29, no. 1, p. 13, 1992.
- [19] S. J. M. Bamberg, a Y. Benbasat, D. M. Scarborough, D. E. Krebs, and J. a Paradiso, "Gait analysis using a shoe-integrated wireless sensor system," vol. 12, no. 4, pp. 413–423, 2008.
- [20] C. B. Redd and S. J. M. Bamberg, "A wireless sensory feedback device for real-time gait feedback and training," *Ieee-Asme Trans. Mechatronics*, vol. 17, no. 3, pp. 425–433, 2012.
- [21] M. Chen, B. Huang, and Y. Xu, "Intelligent shoes for abnormal gait detection," *Proc. - IEEE Int. Conf. Robot. Autom.*, pp. 2019–2024, 2008.
- [22] A. Nsenga Leunkeu, T. Lelard, R. J. Shephard, P. L. Doutrelot, and S. Ahmadi, "Gait cycle and plantar pressure distribution in children with cerebral palsy: Clinically useful outcome measures for a management and rehabilitation," *NeuroRehabilitation*, vol. 35, no. 4, pp. 657–663, 2014.
- [23] A. Rampp, J. Barth, S. Schülein, K. G. Gaßmann, J. Klucken, and B. M. Eskofier, "Inertial sensor-based stride parameter calculation from gait sequences in geriatric patients," *IEEE Trans. Biomed. Eng.*, vol. 62, no. 4, pp. 1089–1097, 2015.
- [24] B. Mariani, M. C. Jiménez, F. J. G. Vingerhoets, and K. Aminian, "On-shoe wearable sensors for gait and turning assessment of patients with parkinson's disease," *IEEE Trans. Biomed. Eng.*, vol. 60, no. 1, pp. 155–158, 2013.
- [25] K. Kong and M. Tomizuka, "A gait monitoring system based on air pressure sensors embedded in a shoe," *IEEE/ASME Trans. Mechatronics*, vol. 14, no. 3, pp. 358–370, 2009.
- [26] I. González, J. Fontecha, R. Hervás, and J. Bravo, "An ambulatory system for gait monitoring based on wireless sensorized insoles," *Sensors (Switzerland)*, vol. 15, no. 7, pp. 16589–16613, 2015.
- [27] S. Crea, M. Donati, S. Marco, M. De Rossi, and C. M. Oddo, "A wireless flexible sensorized insole for gait analysis," pp. 1073–1093, 2014.
- [28] R. E. Spatio-temporal *et al.*, "A mobile kalman-filter based solution for the gait

- parameters,” vol. 24, no. 7, pp. 764–773, 2016.
- [29] L. Shu, T. Hua, Y. Wang, Q. Li, D. D. Feng, and X. Tao, “In-shoe plantar pressure measurement and analysis system based on fabric pressure sensing array,” vol. 14, no. 3, pp. 767–775, 2010.
- [30] P. Lopez-meyer, G. D. Fulk, and E. S. Sazonov, “Automatic detection of temporal gait parameters in poststroke individuals,” vol. 15, no. 4, pp. 594–601, 2011.
- [31] F. Kawsar, K. Hasan, R. Love, and S. I. Ahamed, “A novel activity detection system using plantar pressure sensors and smartphone,” pp. 44–49, 2015.
- [32] N. Hegde and E. Sazonov, “SmartStep: A Fully Integrated, Low-Power Insole Monitor,” *Electron. 2014*, pp. 381–397, 2014.
- [33] L. Donovan, M. A. Feger, J. M. Hart, S. Saliba, J. Park, and J. Hertel, “Gait & Posture Effects of an auditory biofeedback device on plantar pressure in patients with chronic ankle instability,” *Gait Posture*, vol. 44, pp. 29–36, 2016.
- [34] Texas Instruments Datasheet, “CD74HCT4067 High-Speed CMOS Logic,” no. July, 2003.
- [35] J. Melorose, R. Perroy, and S. Careas, “Datasheet Arduino Nano,” vol. 1, 2015.
- [36] I. Electronics, “Interlink Electronics Inc., FSR integration Guide and Evaluation parts catalog with suggested Electrical interfaces,” *Version 1.0, 90-45632 Rev. D, 2007.*, vol. 1.0, pp. 1–26, 2007.
- [37] P. Product and K. Features, “nRF24L01+ Datasheet,” *ReVision*, no. March, pp. 1–75, 2008.
- [38] A. Aggarwal, R. Gupta, and R. Agarwal, “Design and Development of Integrated Insole System for Gait Analysis,” in *Eleventh International Conference on Contemporary Computing (IC3), IC3-2018*, 2018, pp. 1–6. (Accepted)
- [39] H. K, J. S, and M. B, “Comparison of gait before and after superficial trunk muscle exercise and deep trunk muscle exercise,” *J. Chem. Inf. Model.*, vol. 27, no. 11, pp. 0–2, 2015.

ANNEXURE

Pressure plots for the remaining subjects.

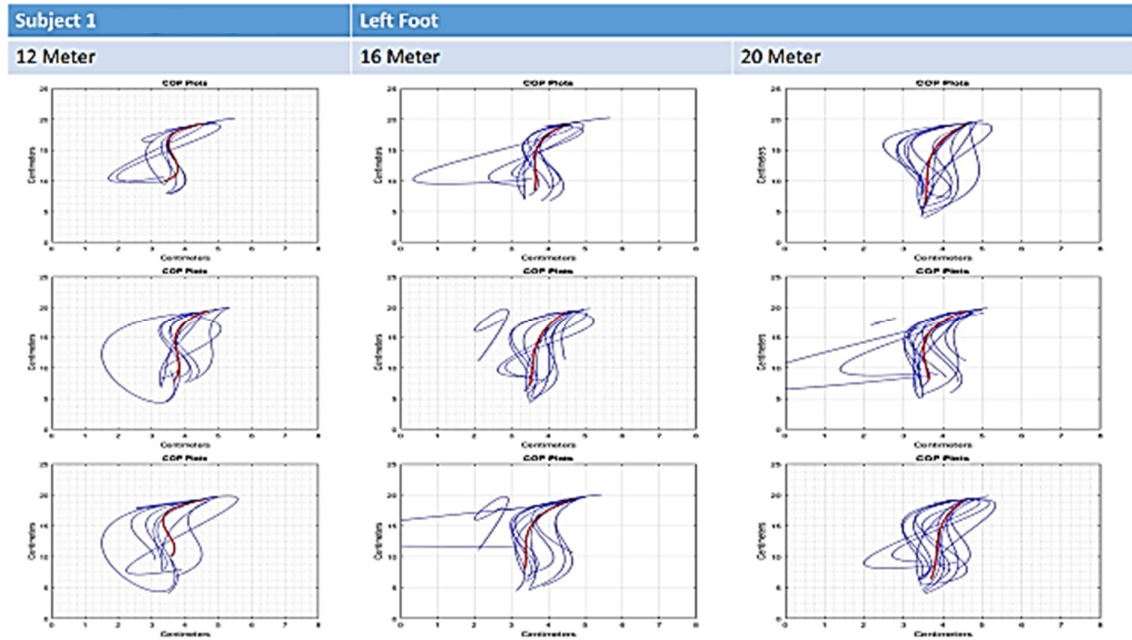


Figure 1: Centre of Pressure Plots for Left Foot of Subject 1

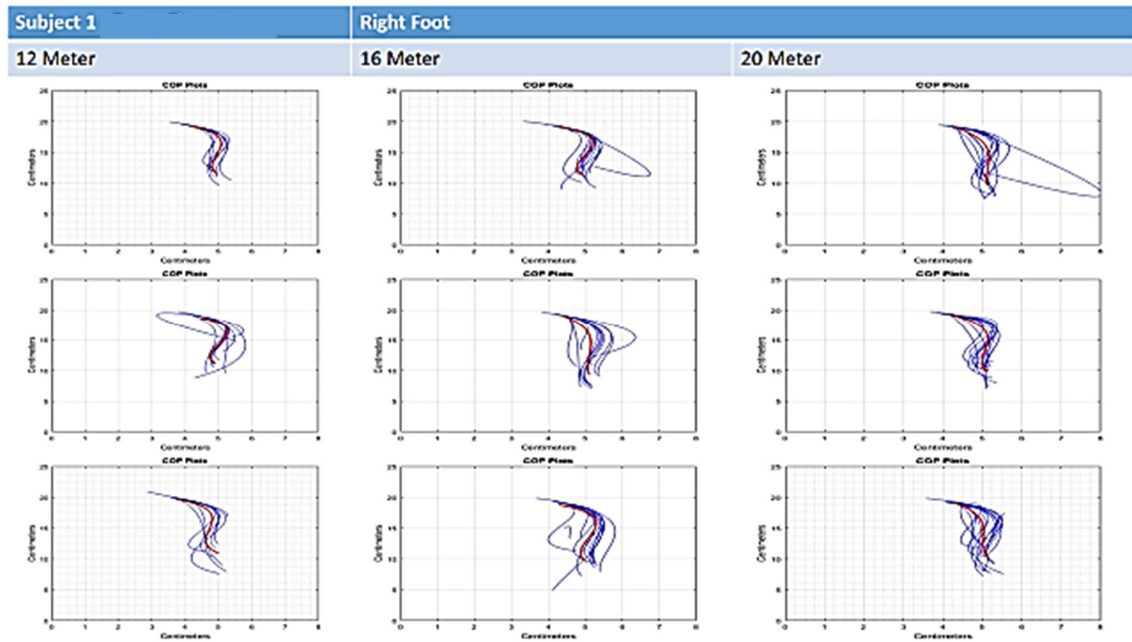


Figure 2: Centre of Pressure Plots for Right Foot of Subject 1

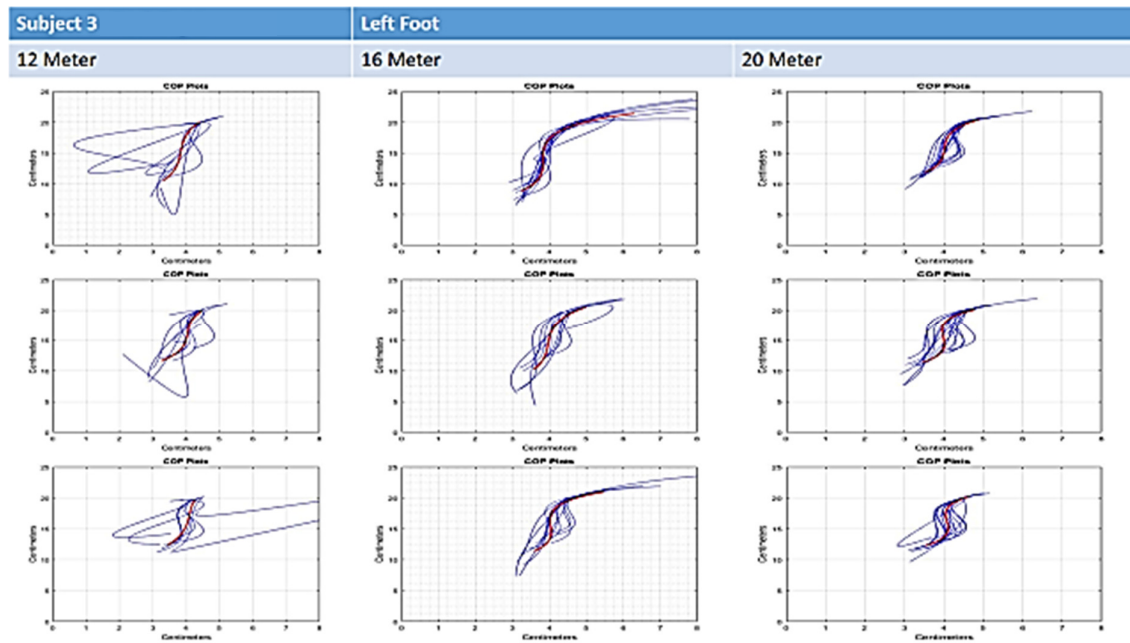


Figure 3: Centre of Pressure Plots for Left Foot of Subject 3

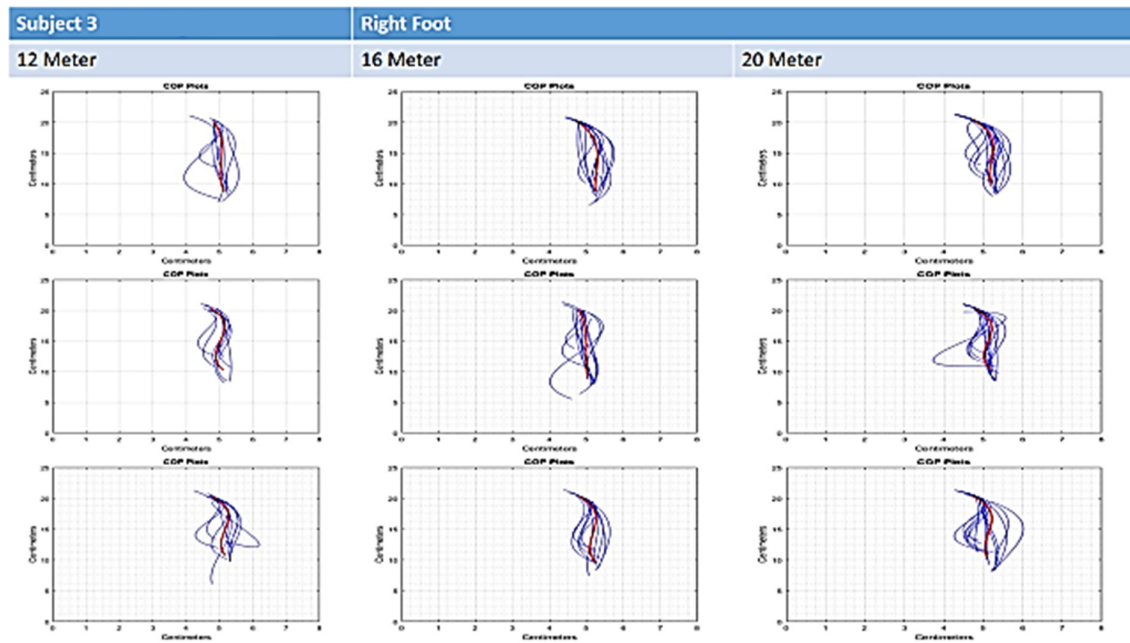


Figure 4: Centre of Pressure Plots for Right Foot of Subject 3

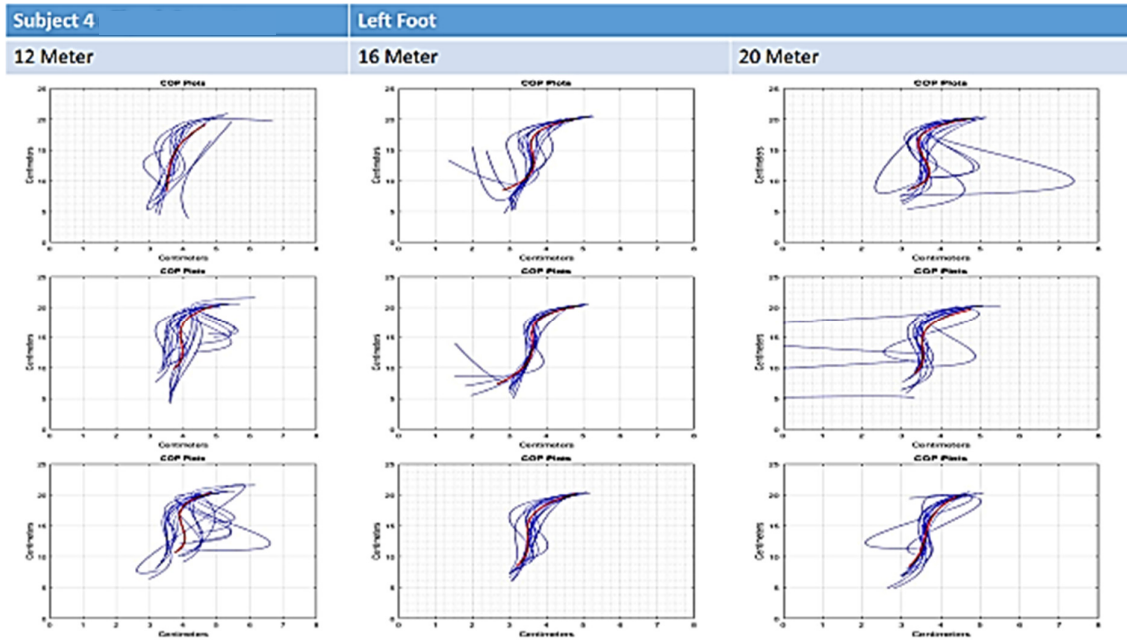


Figure 4: Centre of Pressure Plots for Left Foot of Subject 4

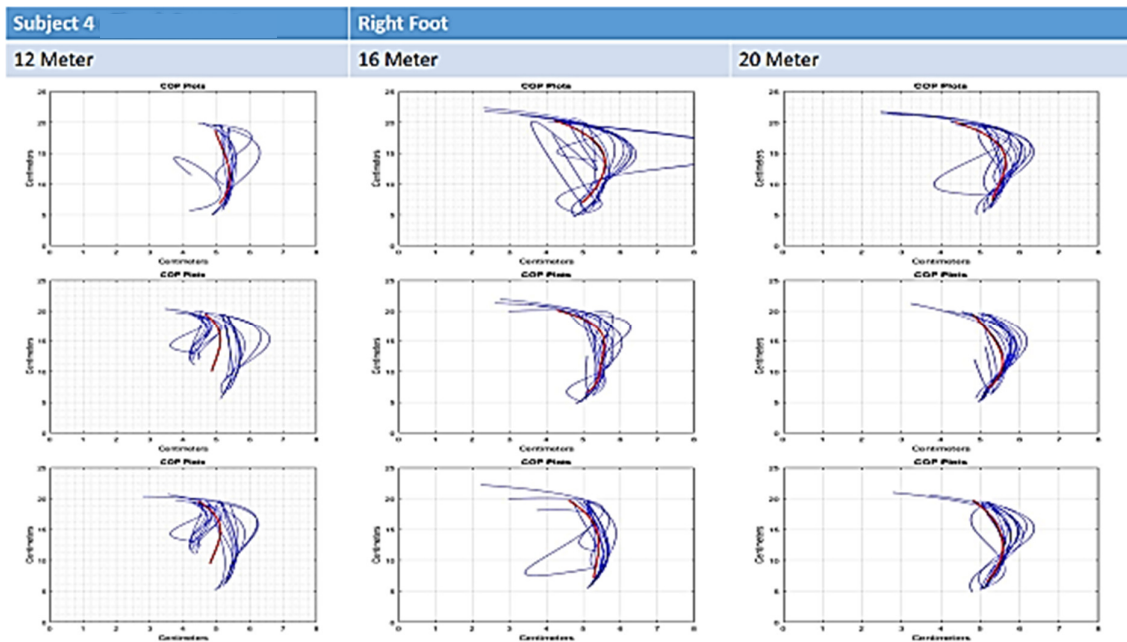


Figure 5: Centre of Pressure Plots for Right Foot of Subject 4

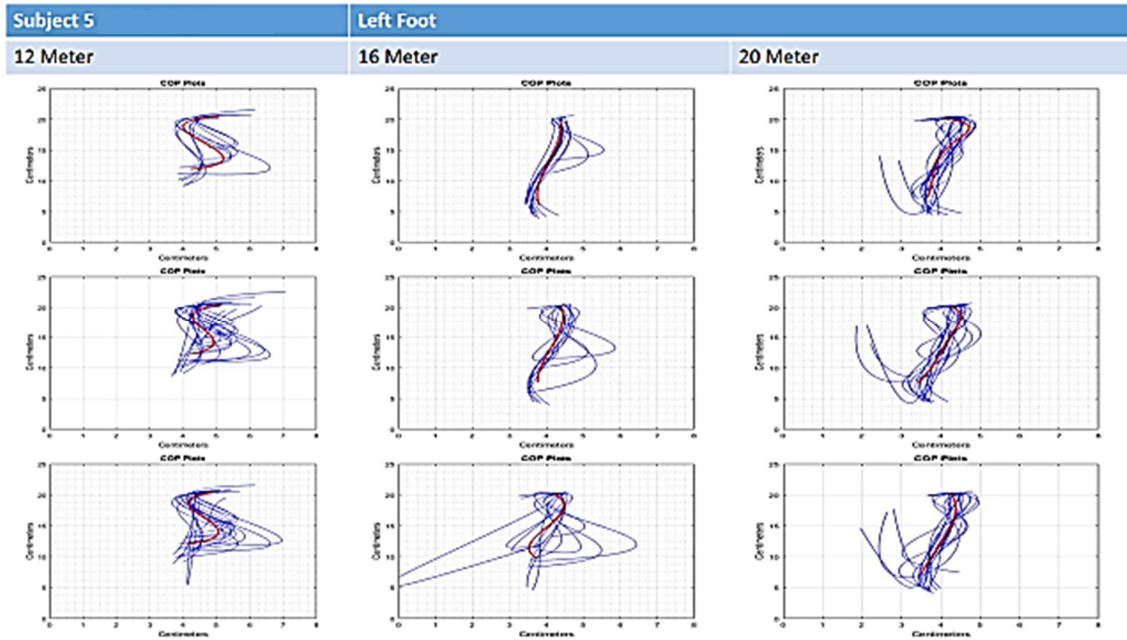


Figure 6: Centre of Pressure Plots for Left Foot of Subject 5

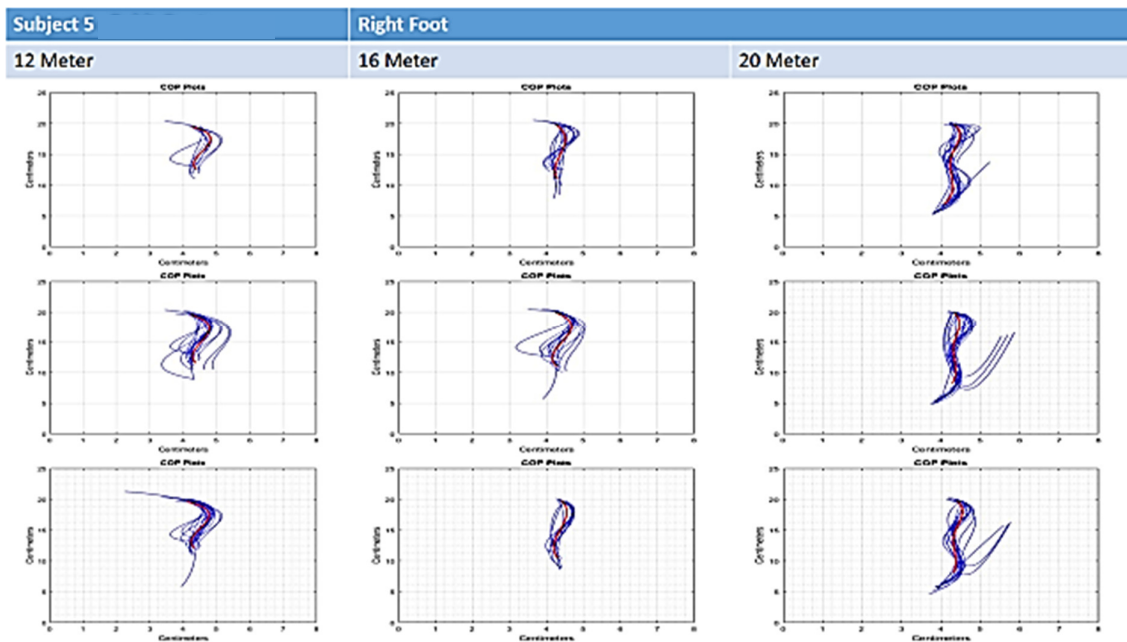


Figure 7: Centre of Pressure Plots for Right Foot of Subject 5

Demographics Table of the subject

Subject	Age	Gender	Weight (kg)	Height (cm)	Leg Length (inch)	Leg Length below Knee (inch)	Leg Length above Knee (inch)
1	30	Male	65	178	34	20	14
2	24	Male	54	165	35	21	14
3	29	Male	88	177	36	20	16
4	29	Male	80	173	32	19	13
5	32	Male	76	170	31.2	18	13.2